EXPERIMENTAL INVESTIGATIONS ON PERFORMANCE OF LINE COMMUTATED INVERTER FED RELUCTANCE MOTOR DRIVE

A DISSERTATION

submitted in partial fulfilment of
the requirements for the award of the degree
of
MASTER OF ENGINEERING
in
ELECTRICAL ENGINEERING
(Power Apparatus and Electric Drives)

By

SWAPAN KUMAR BARAL

DEPARTMENT OF ELECTRICAL ENGINEERING
UNIVERSITY OF ROORKEE
ROORKEE-247667 (INDIA)

February, 1988

CANDIDATE'S DECLARATION

I hereby, certify that the work which is being presented in the dissertation entitled, 'EXPERIMENTAL INVESTIGATIONS ON PERFORMANCE OF LINE COMMUTATED INVERTER FED RELUCTANCE MOTOR DRIVE', in partial fulfilment of the requirements for the award of the degree of MASTER OF ENGINEERING in ELECTRICAL ENGINEERING with specialization in POWER APPARATUS AND ELECTRIC DRIVES, submitted in the Electrical Engineering Department, University of Roorkee, Roorkee [India], is an authentic record of my own work carried out for a period of about six months from August, 1987 to February 1988, under the supervision of Dr. Bhim - Singh, Lecturer, Electrical Engineering Department, University of Roorkee and Sri S.P.Srivastava, Lecturer, Electrical Engineering Department, University of Roorkee, Roorkee, India.

The matter embodied in this dissertation has not been submitted elsewhere for the award of any other degree or diploma.

DATED 20.2.88

[SWAPAN KUMAR BARAL]

This is to certify that the above statement made by the candidate is correct to the best of our knowledge.

20.2.88

[Sri S.P.SRIVASTAVA]
LECTURER
ELECTRICAL ENGINEERING
DEPARTMENT
UNIVERSITY OF ROORKEE
ROORKEE-247667, INDIA

[DR. BHIM SINGH]
LECTURER
ELECTRICAL ENGINEERING
DEPARTMENT
UNIVERSITY OF ROORKEE
ROORKEE-247667,INDIA

ACKNOWLEDGEMENTS

It is a matter of great pleasure for me to express my respect and sincere gratitude to Dr. Bhim Singh, Lecturer, Department of Electrical Engineering, University of Roorkee, Roorkee and Sri S.P.Srivastava, Lecturer, Department of Electrical Engineering, University of Roorkee, Roorkee for their valuable guidance and suggestions althroughout the dissertation work which led to a successful end of this effort and fulfillment of desired objective.

I pay my respect and thanks to Dr. P.Mukhopadhyay, Professor and Head, Department of Electrical Engineering, University of Roorkee for always encouraging me during the entire course of study. I am really overwhelmed by his kind cooperation, guidance and help at different times. I am very much greateful and thankful to faculty members Prof. D.R.Kohli, Prof. V.K.Verma, Prof. R.B.Saxena, Dr. S.P.Gupta, Sri Pramod Agarwal, of the Department of Electrical Engineering, University of Roorkee, for their kind cooperation and help time to time. I feel myself fortunate to have such persons as my teachers.

I would like to thank Mr. S.Giri of the P.G.Machine laboratory for always offering his cooperations during my dissertation work. I also acknowledge and will always remember the help received from the staff members of workshop and all laboratories.

I cannot find suitable language to express my sincere thank to my friends Ram Krishna and Debasish for helping me at the last stage of work.

[SWAPAN KUMAR BARAL]

ABSTRACT

A variable speed ac drive is now found to be most suitable with line commutated inverter system. Therefore, in this dissertation this scheme has been used for the reluctance motor drive to experimentally investigate the performance of the system. In this scheme 3-phase uncontrolled rectifier bridge in combination with a 3-phase auto-transformer converts fixed frequency and voltage a.c. supply into variable d.c. voltage which is then fed to inverter bridge operating in line commutation mode. Terminal voltage sensing method has been adopted to realise the commutation of thyristors and terminal capacitors have been used to supply the lagging reactive power needed for motor and inverter.

An analysis is also made on the basis of a developed analytical model. In order to obtain analytical results, computation with the help of computer has also been done. In experimentation and computation the steady state performance of the system has been investigated. The starting methods have also been discussed. The performance of the system under varied conditions are observed which are elaborated. On the basis of the experimental as well as computed results, the system's feasibility is predicted. The effect of variation of d.c. link voltage V_d and terminal capacitor C on speed control over a wide range has been observed. The validity of the analytical approach is also established by comparing the computational results with experimental ones.

NOMENCLATURE

The full meanings of the symbols used in the present work are listed below in detail -

C	Capacitance
E_m	Peak value of phase voltage
F	per unit frequency
I, I_m	motor current under loaded condition
I_o	no load motor current
I_1, I_I	inverter current
I_d	d.c.link current
m	number of phases
P_{fm}, P_{fI}	power factors of motor and inverter respectively
P_I, P_o	motor input and output power respectively
P_{OM}	maximum output power of motor
P_L	no load losses of the motor
r_a	armature resistance per phase of the motor
T	torque
V, V_P	a.c. side inverter voltage per phase
V_d, V_{dc}	d.c. link voltage
X_c	p.u reactance of capacitor at base frequency
X_d	direct-axis reactance of the motor
X_q	quadrature -axis reactance of the motor
α	firing angle
β	inverter angle of advance

ϕ	power factor angle
δ_{oR}	load angle for any output power
δ_{max}	load angle for maximum output power
n_s	overall system efficiency
n_m	motor efficiency

CONTENTS

	PAGE NO
Candidate's Declaration	(i)
Acknowledgements	(ii)
Abstract	(iv)
Nomenclature	(v)
APTER-I INTRODUCTION	1
1.1 General	1
1.2 Literature Survey	6
1.3 Scope of Present Work	11
APTER-II DEVELOPMENT OF THE SCHEME	14
2.1 Introduction	14
2.2 Principle of Operation	14
2.3 Starting Method of the Motor	15
2.4 Description of System with Design Features	18
2.5 Results and Discussion	25
2.6 Conclusions	25
APTER-III EXPERIMENTAL INVESTIGATIONS ON STEADY STATE PERFORMANCE OF THE SYSTEM	27
3.1 Introduction	27
3.2 Experimental Set Up	28
3.3 Experimentation	28
3.4 Results and Discussions	29
3.5 Conclusions	34
APTER-IV STEADY STATE ANALYSIS OF THE SYSTEM	36
4.1 Introduction	36
4.2 Analytical Model	37
4.3 Computation of Performance Characteristics and Their Experimental Verification	43

4.4 Discussions on Results 45

4.5 Conclusions 48

CHAPTER - V CONCLUSIONS AND SUGGESTIONS FOR FURTHER WORK 50

5.1 Main Conclusions 50

5.2 Suggestions for Further Work 52

BIBLIOGRAPHY

CHAPTER - I

INTRODUCTION

1.1 General

The d.c. machines are now being replaced by their a.c. counterparts in industrial applications due to number of advantages found in the latter. In spite of this fact, the d.c. machines, until recently, was an attraction and choice as they can serve the purpose of speed control over a wide range. The problem associated with the mechanical commutator- brush arrangement in d.c. machines is that it limits the armature current rating and consequently the power output. It is costlier, require regular maintenence and also not suitable in dusty and explosive environments.

The introduction and development of power semiconductor devices and their application for speed control of ac motors has brought significant changes in the concept of drives. Moreover, the ac motors themselves have some excellent merits e.g. ruggedness, simplicity, low cost etc. in case of induction motor and constant speed operation with high power factor etc. in case of synchronous motors. The investigation of current source inverter fed induction motor were resulted in the first ac motor drive which enhanced all the superior properties of ac motor. For some applications, ac drives using inverter fed synchronous machines provides precise simultaneous speed control as well as constancy of speed.

Although a.c.motor has number of advantages including lower cost in comparison with d.c. motors. But the design and manufacture of solid-state variable speed a.c. drive is expensive and complex as compared to that for the d.c. motor. The operation of control equipment is also complicated for a.c. drives.

In the family of a.c. motors, the reluctance motor has attracted attention of researchers [1-8] for some applications because it provides perfectly constant speed like synchronous motor while maintaining the robustness similar to cage induction motor. The reluctance motor is driven by reaction torque due to pole saliency and runs at synchronous speed. It requires no d.c. excitation and is pulled into synchronism automatically. They are cheap,robust and reliable. Because of this feature, the reluctance motor has its application in glass, fiber, pulp and paper industries, for precision control of machine tools, positioning the control rods of neuclear reactors and drives for textile machinery which are completely synchronised under variable speed operating conditions [1,2]. Moreover, with the development of modern solid-state power supplies the demand for variable speed synchronous drives has increased manifold.

A solid state a.c. drive consists of a power conversion unit and control circuitry. Power conversion may either of single stage conversion or of two stages of conversion of voltage and frequency. Of the different types of conversion techniques the only applicable for reluctance motor is frequency control. In variable frequency operation, the motor terminal voltage is also proportionally changed to maintain the necessary air-gap flux. This can be achieved either in single stage such as in cycloconverter or in two stages i.e. independent voltage and frequency control such as in d.c. link inverters [9-16].

A cycloconverter converts fixed frequency a.c. power supply to a variable voltage and frequency in single step conversion process. Due to natural commutation, the operation of cycloconverter is reliable and it also has the inherent capability of regeneration. However, the output contains complex harmonic pattern and it has inherently low power factor of supply and limited frequency range (up to maximum one third of supply frequency). It also requires the large number of components and their complicated control circuitary.

D.C.link inverters are two stage conversion schemes, first converting fixed frequency input to controlled d.c. voltage, which is further converted to produce variable frequency supply for the motor. This d.c. link inverters are of three types-

(i) Voltage Source Inverter (VSI)

(ii) Current Source Inverter (CSI)

(iii) Line Commutated Inverter (LCI)

The voltage source inverters merely changes line voltage and frequency to an adjustable voltage and frequency which is applied to the motor. The VSIs are of two catagories-square wave inverters and pulse width modulated (PWM) inverters. The formar has an undesirable effect- the voltage waves have large number of lower order harmonics which may result in high machine heating at low speed and torque pulsations. The PWM inverters have less harmonics but inverter efficiency is reduced due to higher rate of commutation. The control circuit and commutation are also complex resulting in higher cost. However for low to medium power applications, these commutation circuits can be avoided if the thyristors are replaced by power transistors, GTO thyristors or power MOSFET [16]. These inverters are suited in that case for group drive applications.

In a current source inverter, a regulated d.c. link current is maintained through a bridge rectifier and d.c. link filter choke. The attractive features like simplicity, greater controllability and regenerative capability obtainable in this method together with ease of protection are now widely recognised. By limiting the d.c. current to a safe value the inverter components are prevented from experiencing excessive current and thus remains safe. The commutation losses are less than that in VSIs and its commutation is fail safe [17,18]. It has also been observed that a wide range of speed control can be achieved and regeneration is possible with CSI.

The line commutation is the simplest among all the commutation methods. The process of transferring current from one conducting thyristor to the next, in a rectifier bridge, occurs naturally and automatically in an a.c. system when the anode potential of the incoming SCR is more than that of the conducting SCR. This sequential commutation obtained naturally from a.c. line voltages easily supersedes expensive forced-commutation method. The scheme requires no extra commutating components and the firing circuit is comparatively simpler.

It is, therefore, possible to overcome some of the drawbacks associated with cycloconverter and d.c. link forced commutated inverters by using the line commutated inverter (LCI). The absence of the forced commutation makes the operations of LCI simple, reliable, efficient and cost effective. It requires simple trigger scheme [11,19] and low cost converter grade SCRs may be used. Because of the important features of LCI, it has been exploited by large number of investigators for variable frequency operation of synchronous motor [20-30] and induction motors [31-34]. The LCI fed synchronous motor system is also called d.c. commutatorless motor and provides the characteristics like d.c. shunt and series motors. A need is, therefore, felt to exploit the advantages of LCI for the development of an alternative variable frequency source to control the speed of a robust and brushless system a.c. synchronous motor. With this view, an attempt is made in this investigation to design and develop a d.c. link line commutated inverter for a reluctance motor drive.

1.2 Literature Survey

Alongwith the improvements in semiconductor thyristor technology, the numerous efforts have been made and are still being made to investigate its successful applications to variable speed a.c. motor drives [35-37]. Moreover, with solid state modules, the demand for variable speed synchronous drives has increased tremendously. The reluctance motors are being widely used for the purpose because they offer the possibility of precise speed control, position control and also synchronisation between individual drive points in multimotor applications. A large number of attempts are made on the design, development, theory and analysis, of reluctance motors [1-8] to improve their starting and steady-state performance.

Uezato [1] studied the characteristics of solid rotor three phase reluctance motors and found that if short circuit windings are attached to salient poles it increases the motor torque over entire slip range and increases the pull-in torque. He also concluded that a solid rotor reluctance motor with short circuit winding is sufficiently practical.

Lawrension and Agu [2] made an attempt to improve the performance of reluctance motor in terms of power factor and output torque to make them attractive as constant speed drives. They found that to achieve high output torque and power factor it is necessary for the direct-axis reactance to be made as large as possible whilst the quadrature-axis reactance be made as small as possible. M.H. Nagrial and P.J.Lawrenson [3] have studied both the asynchronous and synchronous aspects of performance of reluctance machine together to attempt to predict optimum parameter combinations, for an overall optimum design with optimum asynchronous and synchronous performance. P.J.Lawrenson and S.K.Gupta [4] developed a segmental type rotor construction of reluctance motor in which complexity of design was avoided and saliency ratio was increased to such a level that utilisation in practice is possible. Mohamadien, Hasan and Osheiba [5] improved the design of motor without any need of extra cage windings. Starting in this case is achieved by virtue of the induced currents in the rotor solid body. Housinger [6,7] innovated a simple but elegent method to find out the direct and quadrature-axis reactances and losses of reluctance motor by no-load and load tests, where the parameters being a function of supply voltage (and frequency). Later on he derived equations, to describe the steady state performances of reluctance machines, from phasor diagrams with the help of parameters - X_d, X_q

armature resistance r_a and no-load loss Uezato and Ueda [8] observed relation that exists between the performance of a solid rotor reluctance with its parameters. They investigated the effect of parameter changes on the performance of the motor, essentially to be considered while designing the motor. They found that steady-state stability of small solid rotor three phase reluctance motor is effected by the changes in machine parameters.

In the light of its specific applications described earlier in this chapter, the reluctance motor's characteristics which were utilised in these applications are adaptibility to position or speed control or a combination of both, using variable frequency or switched supplies, together with the capacity to deliver full torque at all speeds. These characteristics are extremely valuable and it must be considered particularly in view of the developments in the field of static frequency changers, so that the use of reluctance machines for different applications may be made simple and cost effective.

Exhaustive literature survey on variable speed a.c. motor drives reveals that lot of research work have been done on this subject. Since in recent past, synchronous motor operating with LCI has attracted wide attention and quite a large number of efforts have been made to find its feasibility and applications. It is also used to control the speed of case inductor motors [31-35].

K.Phillips [17] observed that with voltage source inverter, unusual load variations, can and often do, push the induction motor to its breakdown point or causes regeneration to occur in the inverter by overhauling the motor and in either case, resulting in untimely shutdown or damage to the motor or inverter. He found that current source inverter gives this drive a rugged nature. Slemon, Dewan and Wilson [18] showed that CSI fed synchronous motor drives provide some feature that make them preferable to CSI fed induction motor drives. They also found that the former is free from the instability or sponteneous oscillation which characterize voltage fed synchronous motor at low voltage and frequency. Venkataraman and Ramaswami [20] have discussed generalised inverter fed synchronous motor drive and concluded that when the motor terminal voltages are to be used for commutation of inverters, the currents in phases lead the corresponding voltages. Hence the field has to be sufficiently excited so that even for maximum expected load on motor, the motor operates at leading power factor. Williamson, Issa and Makky [21] established the advantages of natural commutation over forced commutation. They also preferred rotor position sensor scheme to referenced a.c. terminal voltage for getting firing signal to control the inverters. Since, according to them, this avoids the problems associated with wide frequency variation and high harmonic contents. Cornell and Novotny [22] have successfully explored the method of commutation of Thyristors by armature induced voltage of a synchronous motor instead of rotor position sensor at higher speeds. They observed that this type of commutation is possible as long as power factor angle is a lead angle and is greater than the commutation angle. Le-Huy, Jakabonicz and Perret [23] have implemented. This technique in a microcomputer based system. Davoine, Perret and Le-Huy [24] made an effort to develop some schemes of commutation by armature induced voltage at the time of starting and at very low speeds. Rangandhachari et al [25,26] suggested a variable frequency scheme where line commutated inverter acts in combination with synchronous motor (called commutatorless motor) as a source of variable frequency for induction motor. They concluded that though the system is expensive but it works satisfactorily and voltage and current waveforms are free from harmonics and thus brings in reduction in motor heating and torgue pulsations. Ajay Kumar et al [27] has obtained the d.c. series motor characteristics from LCI fed synchronous motor. Rosa [29] developed very systemetic method to determine the necessary ratings and utilization of power circuit components in a machine commutated inverter-synchronous motor drive. Kotaoka et al [30] has analysed the transient performance of self controlled synchronous motor. Walson [31,32], Singh et al [33] and

S.Seong et al [34] have used the LCI to feed cage induction motor for its variable speed operation and they realised the need of lagging reactive power source for the system which was provided by terminal capacitors.

1.3 Scope of Present Work

From extensive and thorough survey of literatures published so far it is apparent that LCI fed synchronous motor has satisfactory steady state performance and therefore may be a suitable choice as variable speed drive. Quite a handful efforts have been made on either LCI fed only induction motor [31-34] or combination of induction and synchronous motor [25-26]. Till now no research work, at all, has been reported on LCI fed reluctance motor, though it is not very much different from other members in the family of a.c. motors. On the contrary its relationship is closer to both synchronous and induction motors. In view of its some advantages and specific applications briefly discussed earlier in this chapter, it was felt necessary to go into detail investigations of variable speed operation of reluctance motor fed from a line commutated inverter.

The investigations are carried out to study the steady state performance of a line commutated inverter fed 3-phase reluctance motor. In this scheme a variable d.c. source for feeding the active power to LCI is obtained using a combination of an autotransformer with uncontrolled bridge rectifier from a three phase fixed frequency and fixed voltage a.c. supply. The reactive power requirement of the motor and LCI is met by connecting the capacitor bank at motor terminals.

The objective of the proposed work can be summerised as follows -

(i) To develop a firing scheme with a view to realize the operation of the 3-phase thyristor bridge for LCI mode.

(ii) To develop an analytical model for the analysis of system performance.

(iii) To measure the X_d, X_q parameters and no-load losses of the machine as a function of applied voltage and frequency to be used in the analysis for both no-load and loaded conditions of the motor.

(iv) To compute the performance of the drive on digital computer using developed model and suitable numerical technique and to compare the computed results with the experimental ones to verify the validity of the proposed approach.

(v) To study the effect of system parameters like d.c. link voltage, terminal capacitor for obtaining wide range of speed control of the drive.

Outline of Chapters.

Among the chapters followed, principle of operation, details of experimental set up and starting methods are described in Chapter II. Thorough experimental investigations, the steady state performance of system is studied in Chapter-III. Analysis of performance of the system and comparison between experimental and analytical results are given in IVth chapter. In the last chapter the main conclusions are enlisted and suggestions for further work are also proposed. The details of machines and ICs used and the listing of developed computer programs are given in the Appendices.

CHAPTER - II

DEVELOPMENT OF THE SCHEME

2.1 Introduction

A detailed and stepwise development of the scheme is discussed here with a view to realise the objective. The essential components of the scheme are mainly two-the power circuit and firing circuit of the line commutated inverter. The latter was designed in such a way that the commutation of thyristors in the power circuit is possible with the help of back'emf'of the motor connected to the output of the inverter. The firing angle range may be controlled between 90° to 180° to obtain inversion mode of operation. The firing scheme elaborated here uses cosine wave crossing technique to generate firing pulses. The system is not a self-starting one. Therefore it has to be started with some auxiliary means. So as a part of principles of operation of the scheme, a detail description of starting method is given here. The performance of firing circuit with the feasibility of LCI operation is also presented.

2.2 Principle of Operation

Block diagram of the system used in this investigation is shown in Fig. 2.1. The system consists of three phase autotransformer, an uncontrolled 3-phase bridge rectifier, a d.c. link filter choke, line commutating inverter, three-phase capacitor bank and three phase reluctance motor coupled

CHAPTER - II

DEVELOPMENT OF THE SCHEME

2.1 Introduction

A detailed and stepwise development of the scheme is discussed here with a view to realise the objective. The essential components of the scheme are mainly two-the power circuit and firing circuit of the line commutated inverter. The latter was designed in such a way that the commutation of thyristors in the power circuit is possible with the help of back'emf'of the motor connected to the output of the inverter. The firing angle range may be controlled between 90° to 180° to obtain inversion mode of operation. The firing scheme elaborated here uses cosine wave crossing technique to generate firing pulses. The system is not a self-starting one. Therefore it has to be started with some auxiliary means. So as a part of principles of operation of the scheme, a detail description of starting method is given here. The performance of firing circuit with the feasibility of LCI operation is also presented.

2.2 Principle of Operation

Block diagram of the system used in this investigation is shown in Fig. 2.1. The system consists of three phase autotransformer, an uncontrolled 3-phase bridge rectifier, a d.c. link filter choke, line commutating inverter, three-phase capacitor bank and three phase reluctance motor coupled

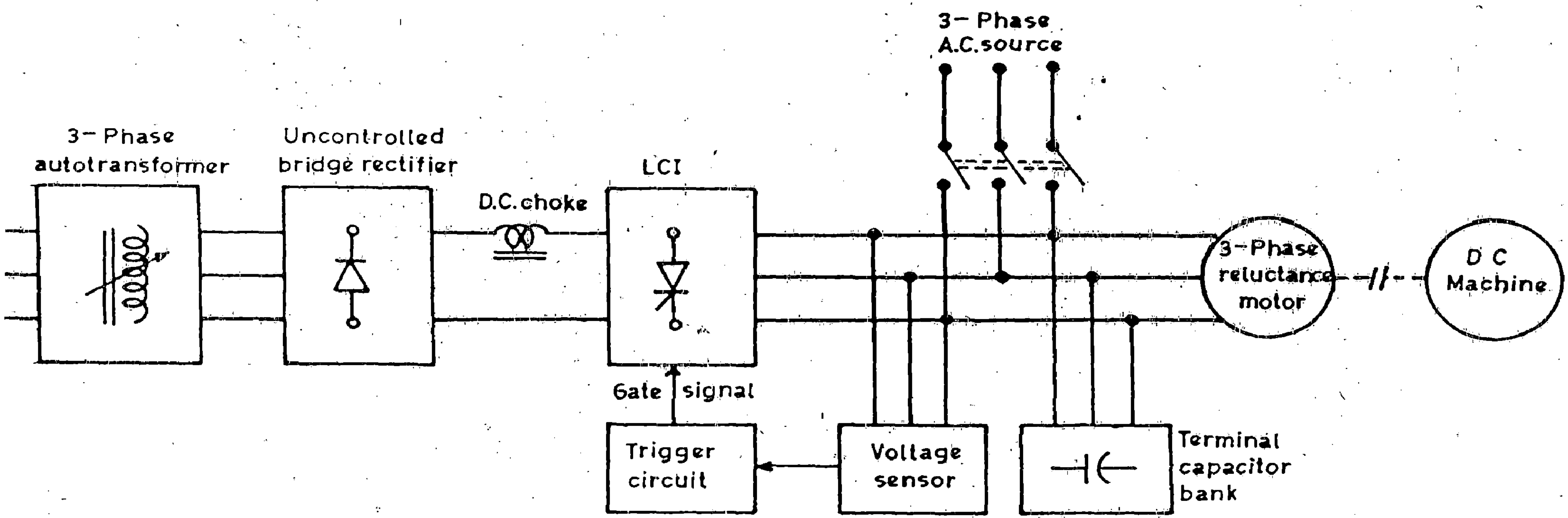

FIG.2.1. BLOCK DIAGRAM OF LINE COMMUTATED INVERTER (LCI) FED RELUCTANCE MOTOR SYSTEM.

with a d.c. motor. The machine terminals are also connected to three phase supply through a switch for starting the system. The three phase autotransformer together with uncontrolled rectifier provides variable voltage d.c. to feed the LCI. The full power circuit is shown in Fig. 2.2. The function of the d.c. link inductor is to smoothout the link current ripples. The flow of power to the motor in LCI mode of operation can be controlled by adjusting the d.c. link voltage and the inverter delay angle. The reluctance motor unlike synchronous motor, cannot be run under leading power factor. Hence the essential need of lagging reactive power for inverter and the reluctance motor is provided by the capacitor bank connected at the motor terminals. Motor terminal voltages are sensed with a voltage sensor to generate firing pulses for firing the thyristors of the inverter bridge. The frequency output of motor or speed of reluctance motor may be controlled by varying d.c. link voltage, value of terminal capacitor and the inverter firing angle.

2.3 Starting Method of The Motor

As the terminal voltage sensing scheme has been opted for firing the thyristors it is evident that at stand still condition of motor, the generated emf of the motor is not present to generate triggering pulses. SCRs will not conduct resulting in non-flow of energy from d.c. side to a.c. side of the inverter. As a result motor cannot be

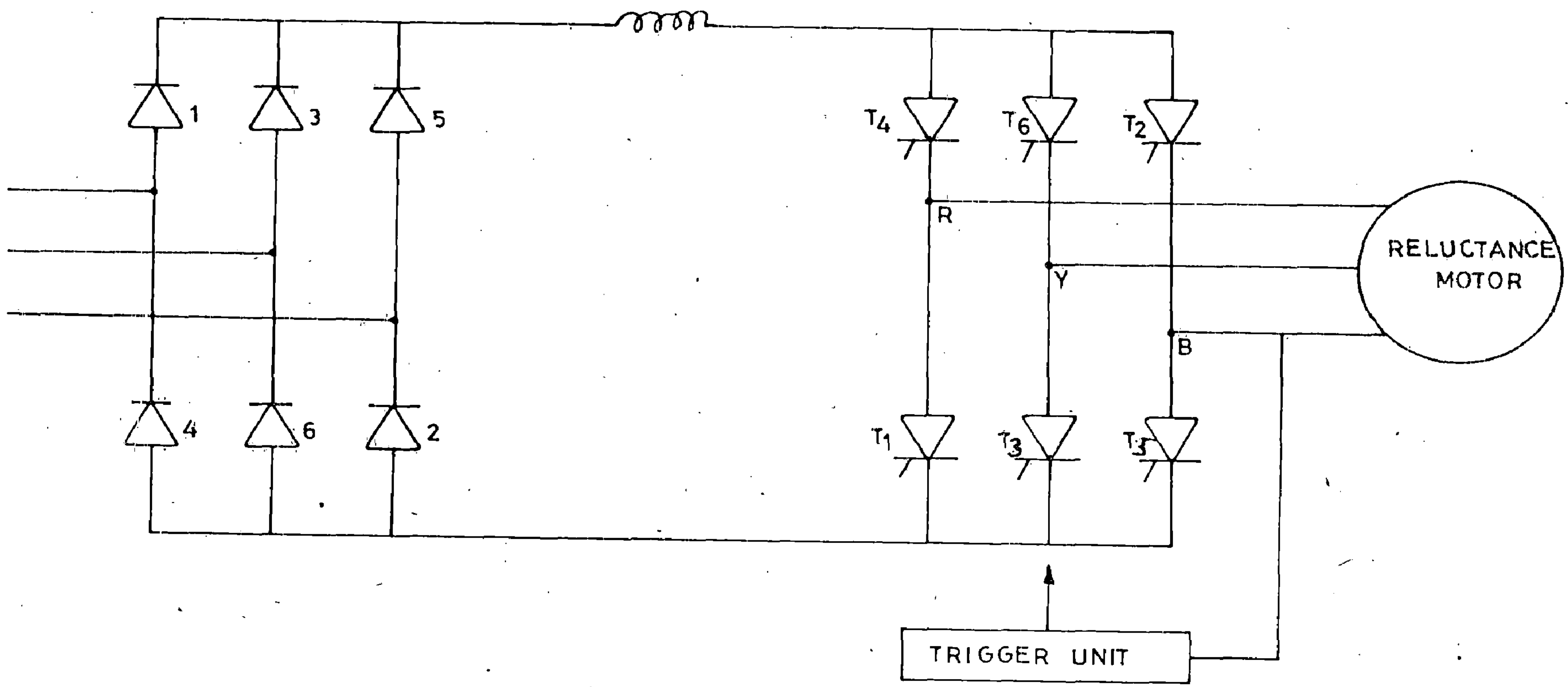

FIG. 2·2—THE PHASE SCR BRIDGE (LINE COMMUTATED INVERTER)

Table 2·1

TIME IN DEGREES	0	60	120	180	240	300
FIRING SEQUENCE	1	2	3	4	5	6
CONDUCTING SCRS	6, 1	1, 2	2,3	3,4	4,5	5,6

started. The shunt capacitor bank supplies the required lagging reactive power when there is the presence of the induced voltages of the reluctance motor across its terminals. So if the motor is pulled into step to provide magnetization as well as to develop sufficient back emf. at the terminals of LCI to commutate the thyristors then active power can flow from the d.c. side. With the help of this real power and the reactive power coming from the capacitor bank, the system starts working.

Two methods can be adopted to accomplish starting of the motor.

2.3.1 Starting from Three Phase Supply

As shown in the block diagram of Fig. 2.1 normal 3-phase supply is given to motor through a switch. Capacitor remains connected to the motor terminals but the inverter remains isolated. The motor is brought to synchronous speed and the inverter terminals are now connected to motor terminals. Generated terminal voltages are by this time become sufficient to produce the firing pulses. Gradually, the power is pushed from the d.c. side of the inverter. At certain stage depending upon the adjustable a.c. supply to the machine terminals it is possible to force the power from d.c. side to a.c. side of the inverter. If all the line currents are same and stable it confirms line commutation alongwith sequential commutation of SCRs as desired. Now the a.c. supply is cut off from the machine terminals. The motor remains continue to run stably with LCI at self adjusted frequency and its no load losses are fed from the d.c. link through inverter.

2.3.2 Starting by a Coupled D.C.Motor

Block diagram of Fig. 2.1 shows a d.c. motor coupled to the reluctance motors shaft. The latter is brought to a suitable speed with the help of d.c. machine acting as a motor and appropriate capacitors being connected to the terminal of the reluctance machine to work as self excited generator.

Inverter terminals are now connected to the machine terminals and firing pulses are thereby generated by the induced emf of reluctance machine. Active power being supplied by the d.c. machine is gradually reduced as active power from the d.c. side of the inverter is increased gradually. When commutation takes place properly power from the d.c. side of the inverter is fed to the reluctance machine and its operation gradually changes from generating to motoring mode. Then the d.c. supply from the d.c. machine is disconnected.

As a matter of fact the d.c. machine coupled to the reluctance motor serves dual purposes. Apart from being an alternate method of starting where its acts as a motor, it is also used to load of the reluctance motor when it acts as a generator. The d.c. voltage generated from d.c. machine can be applied to a suitable load.

2.4 Description of System With Design Features

The diagram of full power circuit is shown in Fig.2.2. It consists of one uncontrolled diode bridge and one controlled thyristor bridge. The design principle of each of them is discussed first and then the design of firing circuit is given in detail.

2.4.1 Selection of Rating of Power Circuit Components

(i) Uncontrolled diode bridge rectifier -

The input to the three-phase diode bridge is considered to be 400V line to line. 50 Hz a.c. The voltage rating of the diodes are expressed in terms of peak inverse voltage appearing across them. Thus if the maximum line voltage is 400V, then peak inverse voltage (PIV) across each diode is

$$PIV = \frac{\pi}{3} V_{do}$$

where,

$$V_{do} = \frac{3\sqrt{2}}{\pi} V_{L-L}$$

$$= \frac{3\sqrt{2} \times 400}{\pi} = 540.2$$

$$\therefore PIV = 566 \text{ volts.}$$

Keeping safety factor of 2 to enable them to withstand sufficient transient overshoot, diodes with 1200 PIV rating has been taken for use. The motor current rating is 2.6A, so under no circumstances, the active load current as well as d.c. link current could have been allowed to exceed 5A. With a safty margin 2, it would have been sufficient to take diodes of 10A rating. Due to easy availability of its range the diodes of 1200V, 16A rating are used.

(ii) Three Phase LCI bridge -

The voltage, current and power rating of the SCRs of this bridge depend on the corresponding rating of the reluctance motor it has to supply. The machine used for this work is 0.5KW motor with 400 V line-to-line supply. So the PIV as calculated in case of diodes is 566V. With a safety factor of 2, the nearest suitable and available 1200 PIV rating was taken. The current rating of the motor is 2.6A. Seldom the motor current was allowed to exceed this limit and even then for very brief duration. Taking the safty factor into account to withstand transient inrush, rating like 10A would have been sufficient for the thyristors. Again due to easy availability of rating of its range. 1200V, 16A rating SCRs were used. Necessary snubber circuits were also provided for (dv/dt) protection of SCRs.

2.4.2. Design and Development of Firing Circuit

(i) Basic principle of firing scheme -

Among the thyristors shown in Fig. 2.2.

T_1, T_2 and T_3 are called positive group of thyristors because they conduct when the a.c. phase voltages become positive, while T_4, T_6 and T_2 are called negative group pf thyristors as they conduct when the supply phase voltages are negative. The inverter operation is to be achieved with a delay angle in the range of 90° to 180° and this has to be materialised with the firing circuit. Six thyristors T_1 to T_6 are to be fired sequentially at an interval of 60° in one cycle of a.c. wave. In each interval a pair of thyristors-one from positive group, the other from the negative group of the remaining two phases, conduct. Table 2.1 shows these combination of thyristors along with firing sequence. So it is apparent that each thyristor is conducting for 120° duration and is turned OFF when the next thyristor of the same group in sequence is gated. Thus the necessary frequency of the gate pulse is six times the supply frequency. The line to neutral and line to line wave-forms are shown in Fig. 2.3 and 2.4 respectively. The reference point of the firing angle (α) can be obtained either from the cross over point of the phases or the zero crossing point of the line voltages. From the Fig. 2.4, when V_{RY} is a positive maximum i.e. $\omega t = 90^\circ$, T_1 and T_6 are conducting and output voltage $V_o = V_{RY}$. When V_{RY} is at negative maximum,

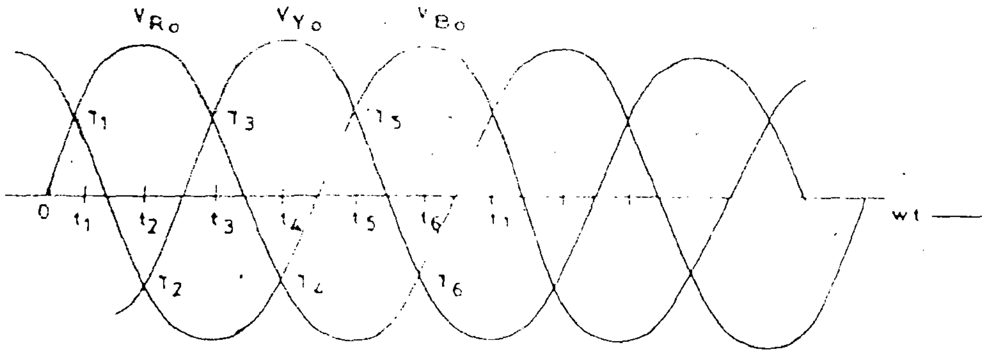

FIG. 2.3 3 PHASE VOLTAGE WAVEFORMS

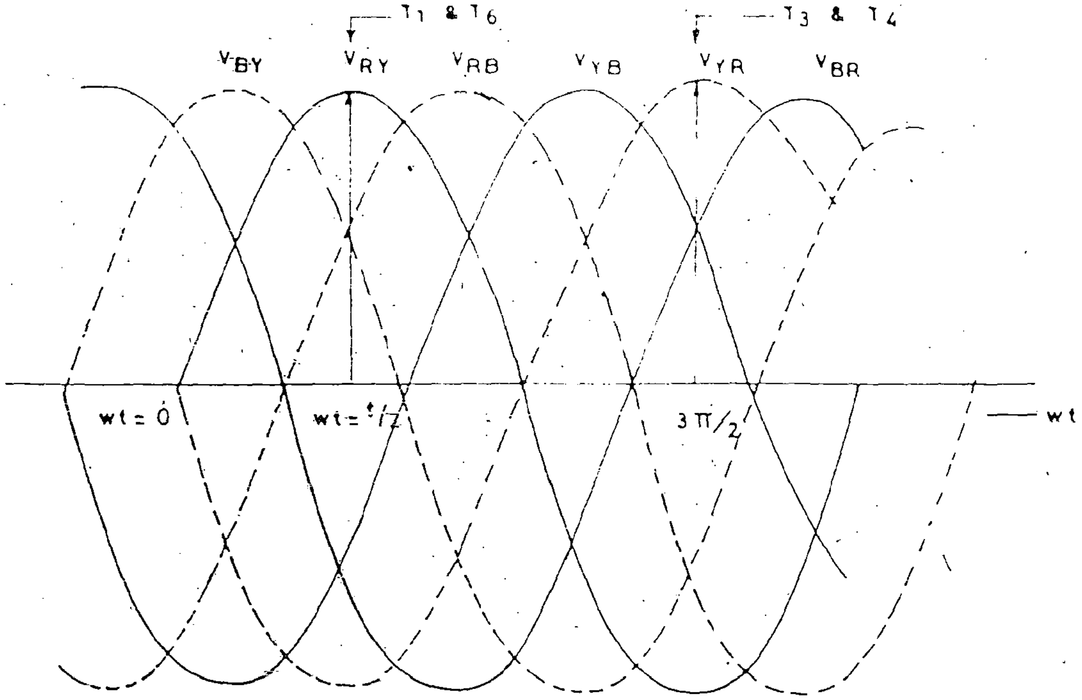

FIG. 2.4. 3 PHASE LINE VOLTAGES

S. NO.	wt = θ	SCR TO BE TRIGGERED	MAX. VALUE LINE VOLTAGE
1	t_1	T_1	V_{RY}
2	t_2	T_2	V_{RB}
3	t_3	T_3	V_{YB}
4	t_4	T_4	V_{YR}
5	t_5	T_5	V_{BR}
6	t_6	T_6	V_{BY}

TABLE NO. 2.2

then T_3 and T_4 are conducting, giving output voltage $V_o = - V_{RY}$ at $\omega t = \frac{3\pi}{2}$. Similarly, for other line voltages, the appropriate pairs to conduct at particular time as it is shown in Table 2.2.

From the waveshape of phase voltages it is apparent that each phase voltage is more positive than the other two for a period of 120^o, which is the interval of two crossover points of two phase voltage waveforms. An uncontrolled diode in place of SCR starts conduction from this point t_1, where $\omega t = 30^o$ and conducts upto $\omega t = 150^o$. So in case of a thyristor this point t_1 is the reference point of thyristor T_1 and accordingly the other points for remaining thyristors.

In a three phase fully controlled converter the relation between d.c. input and a.c. output or vice-versa (depending upon the mode of operation) is given by

$$V_{dc} = \frac{3\sqrt{3}}{\pi} E_m \cos \alpha$$

where E_m is the maximum value of phase to neutral voltage and α is the firing angle of the thyristors. So it is apparent from the relation that as α exceeds 90^o, V_{dc} becomes negative resulting an inverter operation. If a d.c. source of proper polarity is present, power will flow from the d.c. to the a.c. side.

(ii) Details of firing circuit

The block diagram of the firing circuit is shown in Fig. 2.5a. The waveforms corresponding to different stages are shown in Fig. 2.5b. The scheme consists of three step down transformers, comparators, monostable multivibrator, OR gate and pulse amplifier blocks. The complete circuit diagram is shown in Fig. 2.6. Description of function of each stages are detailed below.

<u>Stepdown transformer</u>

To generate the firing pulses the motor terminal voltage sensing scheme is adopted. Since the terminal voltages are always at much higher level, it is essentially necessary to bring it down to a lower level to make compatible to the digital ICs used in firing circuits. For this purpose three stepdown transformers of 400/6-0-6V (i.e. with center tapped secondary) are fabricated. The primary windings are connected in delta and are supplied by the generated terminal voltages at the machine terminals. Six secondary terminals are so arranged as to get six channels of firing pulses for six thyristors. All center tappings are grounded and are connected to the system ground.

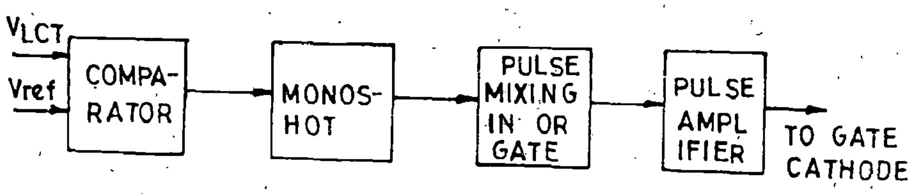

FIG.2·5 a - BLOCK DIAGRAM OF FIRING CIRCUIT

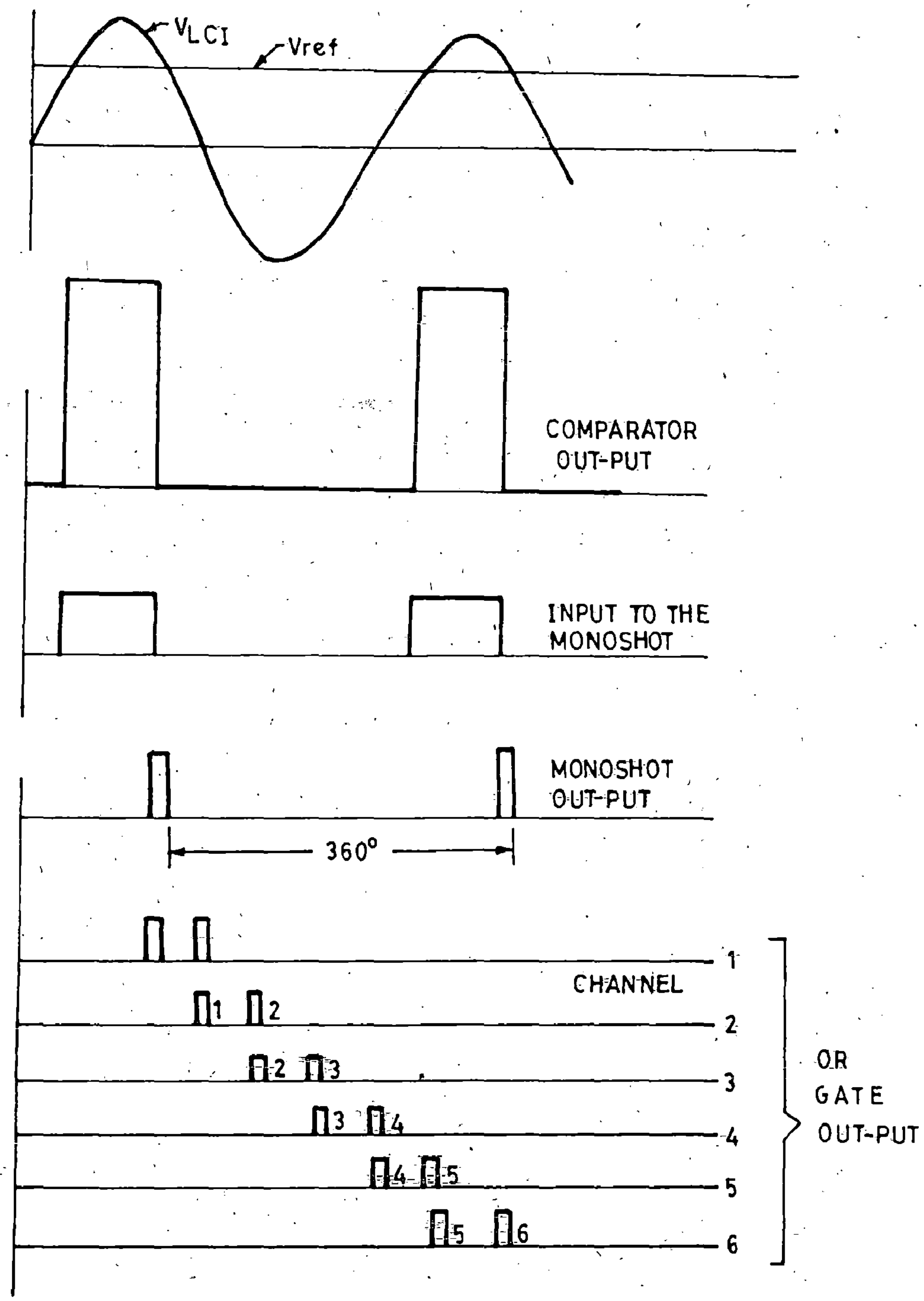

FIG.2·5 b — WAVE FORMS AT DIFFERENT POINTS OF FIRING CIRCUIT

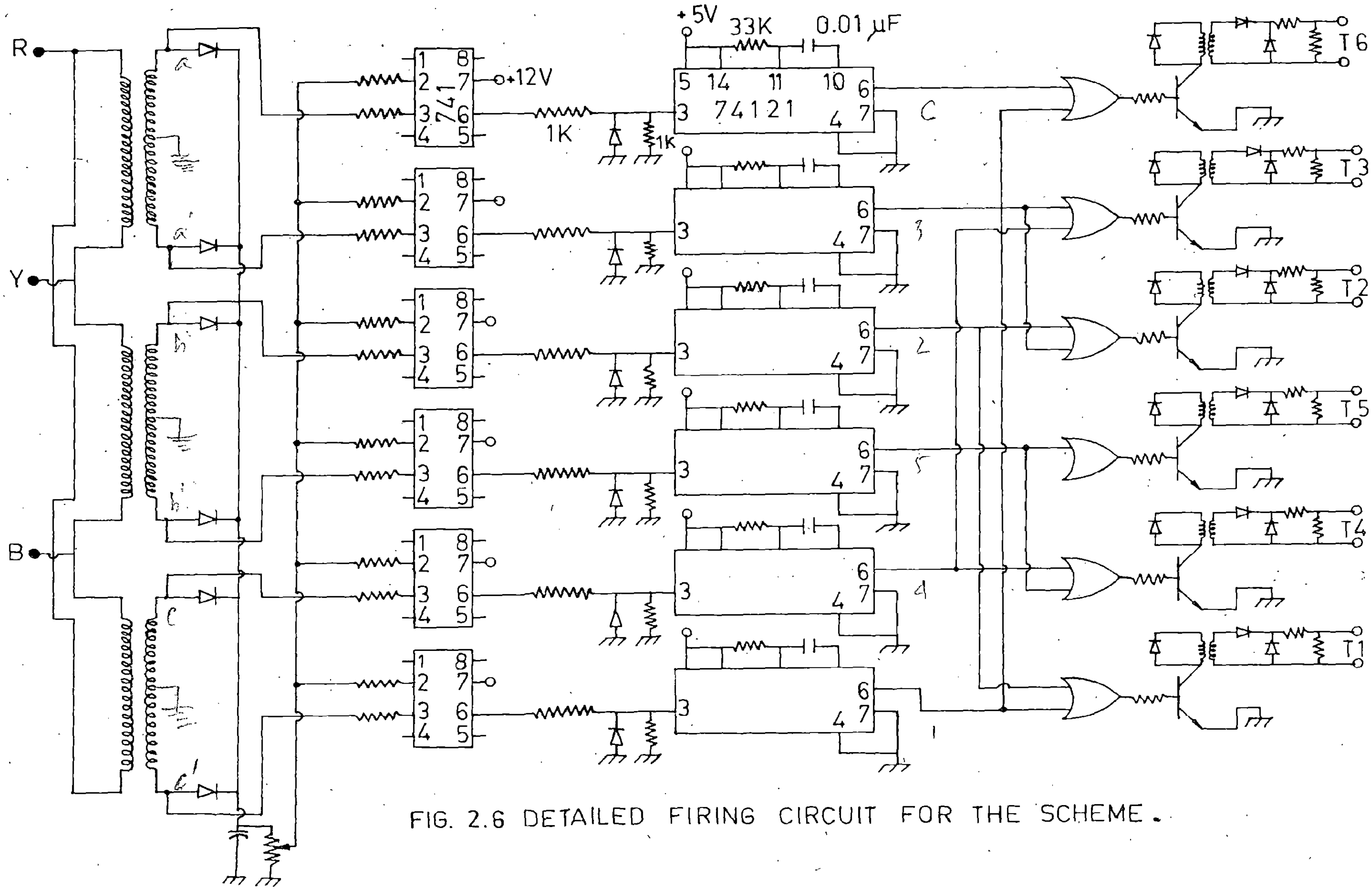

FIG. 2.6 DETAILED FIRING CIRCUIT FOR THE SCHEME.

Comparator

The comparator circuit is made of operational amplifier IC 741. Output of the six secondary terminals of the step-down transformer are given to the non-inverting terminals of each comparator. This a.c. output is to be compared with a d.c. reference voltage given to the inverting terminals of comparators. The output voltage and frequency at the machine terminals and hence at secondaries of the stepdown transformer are not constant. Therefore it is not possible to obtain the same firing angle α with a constant d.c. reference voltage while the frequency and magnetude of the a.c. voltage are changing. Thus to prevent α from changing with frequency variations, the d.c. reference voltage was generated from the terminal voltage of secondary of transformers itself. This is done by rectifying the a.c. output voltages of the secondaries of the step down transformer. The comparator compares the a.c. voltage and the d.c. reference voltage which generate rectangular waveforms.

Monostable multivibrator

The negative part of the rectangular wave cycle is then bypassed using reverse diode connected to the ground. The amplitude level of the (positive portion) wave is then reduced to half, i.e. closer to 5V to make it compatible for the IC74121 being used here as the monoshot. The monoshot produces an output pulse of 0.5 msec. duration using negative edge triggering to produce delay angle 90° to 180° necessary for inverter operation. The elements R and C of the pulse forming circuit are selected as 8.2 K ohm and 0.1 μF respectively.

OR gate

The output of each monoshot is at a phase difference 60° with the adjacent ones corresponding to its original a.c. wave. As each thyristor is to conduct for 120° and it has to be gated twice at the interval of 60°. So each pulse is combined by the OR gate with the pulse 60° ahead of it. The pulse following the main pulse is called the slave pulse. Quad IC 7432 two input OR gate is used for this purpose.

Power amplifier

The pulses generated by the monoshot and then coming out of the OR gate usually don't have sufficient strength to turn the SCRs ON. Therefore, these pulses need to be amplified by an amplifier stage. Transistor SL 100 is used here for this amplification purpose. The gate and cathode terminals of the SCRs are at higher potential of power circuit. Therefore, the control circuit need to be isolated from those. Pulse transformers are used for this purpose. A diode IN4001 is connected across the primary of the transformer to avoid saturation. Another diode is connected in series with the secondary to block negative pulses. The gate is protected against over voltage by connecting a diode across gate to cathode.

The detail pin diagrams of different ICs used and the truth table (where necessary) are given in Appendix -A.

2.5 Results and Discussion

The proposed power and firing circuits have been fabricated and tested for LCI fed reluctance motor system. The corresponding waveforms at different points of the firing circuit are recorded using multichannel storage CRO and are shown in Fig. 2.7a. The waveforms are found to be identical with the theoritical ones shown in Fig.2.5b. The operation of the scheme has been found to be quite stable when control voltage and operating frequency are varied simultaneously. The voltage waveforms at the output of the LCI are shown in Fig. 2.7b. Because of small commutation overlap, the voltage waveforms at motor terminals are found sinusoidal as may be visualised from the Fig. 2.7b.

2.6 Conclusions

Starting with the block diagram of the system. The detail description, development and design of the system has been given. The system is not a self-starting one and hence starting methods have been discussed with sufficient

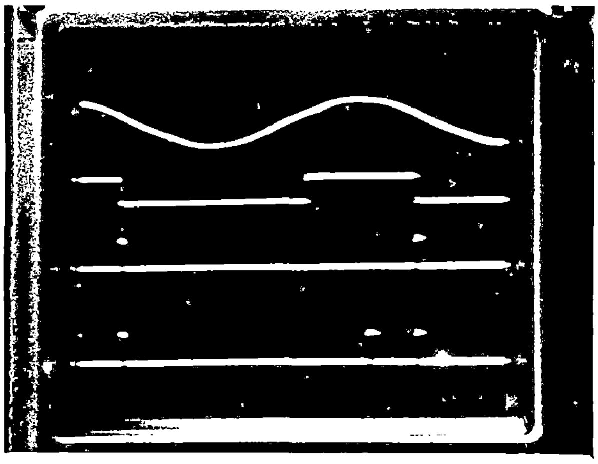

FIG. 2.2a(i)

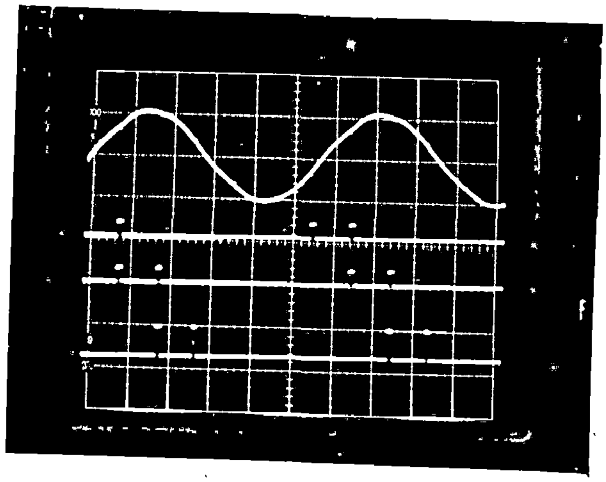

FIG. 2.7a(ii)

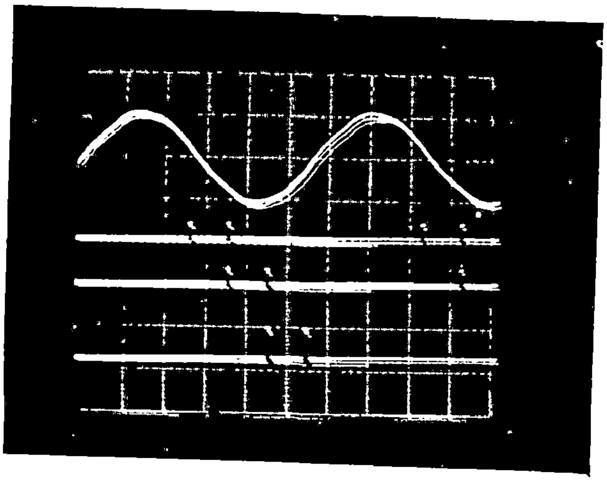

FIG. 2.7a(iii)

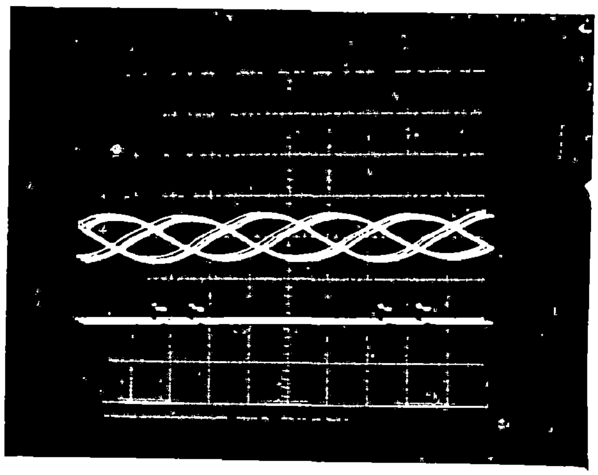

FIG. 2.7b

FIG. 2.7a: WAVEFORMS AT DIFFERENT POINTS OF FIRING CIRCUIT

(i) COMPARATOR, MONOSHOT AND OK GATE OUTPUT

(ii)and(iii) OF GATE OUTPUT OF DIFFERENT CHANNELS

FIG. 2.7b: VOLTAGE WAVEFORM AT THE LCI TERMINAL importance. The indispensibility of the use of terminal capacitors has also been explained. Necessary protective measures have also been taken to save the costly components.

In designing the firing circuit, efforts have been taken to use less number of components resulting in reduction of cost and space for the firing circuit. Each thyristor was tested individually with the firing circuit before going to actual operation. The scheme has been found to work satisfactorily in LCI mode of operation. It is also observed from recorded oscillograms of signals at variaus stages of firing circuit that those are identical to the expected theoritical ones. It is concluded that the developed LCI system provides the pure a.c. sinusoidal variable frequency source for speed control of reluctance motor.

CHAPTER - III

EXPERIMENTAL INVESTIGATIONS ON STEADY-STATE PERFORMANCE OF THE SYSTEM

3.1 Introduction

Exhaustive literature survey reveals that no work has, so far been done on LCI fed reluctance motor. Lot of efforts have been made in case of LCI fed synchronous motor with analog as well as microprocessor based control scheme. In addition to steady state performance analysis, transient and dynamic performances of an LCI fed synchronous motor have been investigated. But the reluctance motor combines some of the advantages of both induction and synchronous motor. So, here, an investigation is made to observe its potentiality and feasibility as a variable speed drive using LCI. The steady state performance of LCI fed reluctance motor drive is studied.

The experimental investigations are made pertaining to the steady state performance of drive under no load and loaded conditions. In LCI fed operation, the speed of the reluctance motor can be varied by varying terminal capacitance, d.c. link voltage and the delay angle of firing, α of LCI. The effect of the value of terminal capacitor and dc link voltage is only studied to obtain wide range control of the drive.

3.2 Experimental Set Up

Fig. 3.1 shows the detail set up for experimentation as well as for starting, provision was made in such a way that the d.c. machine, if used for starting, can later on be used as the load for the load test of the drive. D.C. voltmeter and ammeters are placed in the d.c.link. Three a.c. ammeters of identical rating and scale are placed on inverter output terminals. A three-phase wattmeter was placed at the machine terminals to record the power input to the machine. Voltmeter was placed across the machine terminals. Ammeters are also placed to record the machine line current and capacitor current. D.C.voltmeter was placed accross the load of the d.c. machine and ammeter was placed in series with the load. The lamp load and variable resistors combination is taken as the load. Seperately excited field of the d.c. machine was supplied by the d.c. supply keeping a variable resistance in series with the field.

3.3 Experimentation

Experimentations are done for both no-load and loaded conditions of the drive. In no load test, the terminal capacitance and d.c. link voltage are varied for a wide range of speed control of motor. A descretely variable capacitor bank was used, whose range of

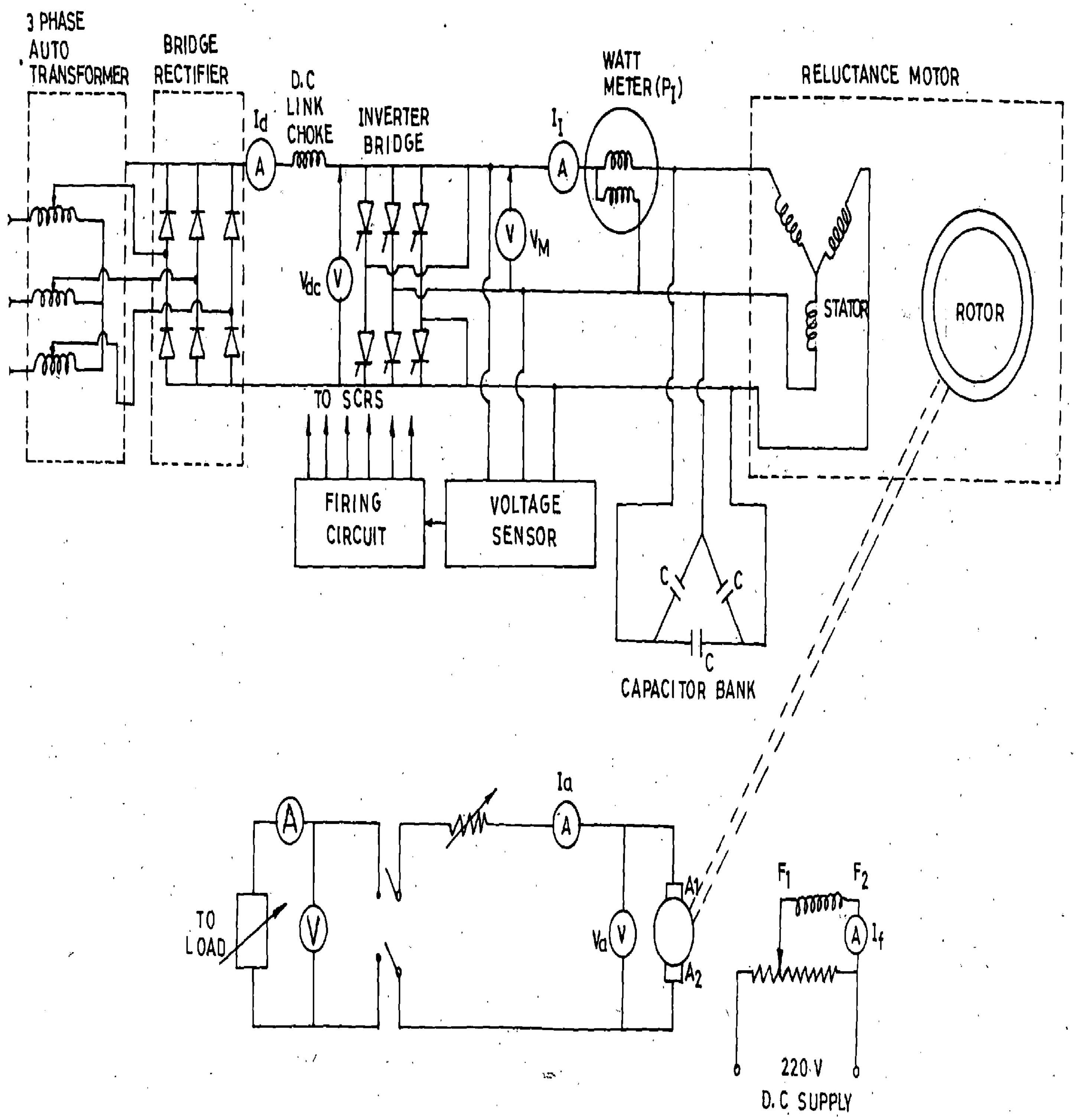

FIG. 3·1–CIRCUIT DIAGRAM OF THE LCI FED RELUCTANCE MOTOR SYSTEM variation was from 10 uF to 80 μF and variation of 10 μF was made. Though the d.c. link voltage may be varied continuously, but it was varied from 100 V to 440 volts, with an interval of 20V. The motor current was a restricting factor which did not permit higher d.c. link voltage for higher capacitences. First a particular capacitance was kept fixed and the d.c. link voltage was varied. The higher range being restricted by motor current, the lower range was tried until the commutation failure. The capacitance is then changed and the process was repeated.

For load tests, four combinations of capacitance and d.c. link voltage were chosen in different speed ranges. These were selected in such a way that in each case the machine operates at rated flux condition. The field of the d.c. machine was excited from the d.c. mains and the machine was run as a generator. With load variation, the excitation of the d.c. field was kept constant. This was done with the help of a variable resistance placed in series with the field. The reluctance motor used for the experiment is of power rating 0.5KW, the details of the reluctance and d.c. machine is given in Appendix - B.

3.4 Results and Discussions

The various test results of LCI fed reluctance motor drive are shown in Fig. 3.3 to 3.5. The following salient features may be observed from the results.

(i) Fig. 3.3a shows the curves of speed versus capacitance for different values of d.c. link voltages. Those curves indicate the effect of changing the capacitance on speed variation. As capacitance is decreased the speed rises while d.c. link voltage was kept fixed. It is also apparent that higher d.c. link voltage cannot be obtained due to limitation from the motor current. The pattern of curves also indicates that the rate of increase of speed is more with smaller values of capacitance i.e. in higher speed range with lower capacitance value and the sensitivity is also higher.

(ii) The effect of variation of d.c. link voltage on the speed for various values of terminal capacitors as shown in Fig. 3.3b. The speed of the motor is seen to be increasing quite linearly with the increase in d.c. link voltage. The rate of increase also appears to be almost identical with different settings of capacitances. At higher values of capacitances the higher d.c. link voltage is not obtainable. While on the other hand with lower capacitances operation is not possible with very lower values of d.c. link voltage. This was a limitation from commutation failure.

However, the important aspect found from the no-load operation is that by varying capacitance and d.c. link voltage, very wide range of speed variation can be obtained. The range of speed control was obtained from 26 percent to 100 percent or from 13 Hz to 50 Hz in terms of frequency. Considering the nature of responses of the speed to the change of d.c. link voltage and capacitance the operation and control of speed at higher region can better be done by changing the value of capacitor. At lower speeds, the d.c. link voltage can be adjusted properly. One interesting feature also comes out, that there is the reduced requirement of capacitance at higher speeds, thus reducing the effective cost of the system.

(iii) Under loaded condition, the torque-speed characteristics are shown in Fig. 3.4a for different conditions of capacitance and d.c. link voltage. It is observed that there is almost no change in speed with the variation of load. It was also observed that for a particular combination of d.c. link voltage and capacitance the no-load speed is also very close to the speed under loaded conditions. With low d.c. link voltage and higher capacitance the speed obtained at no-load is in the lower range. It is evident from the curves that with

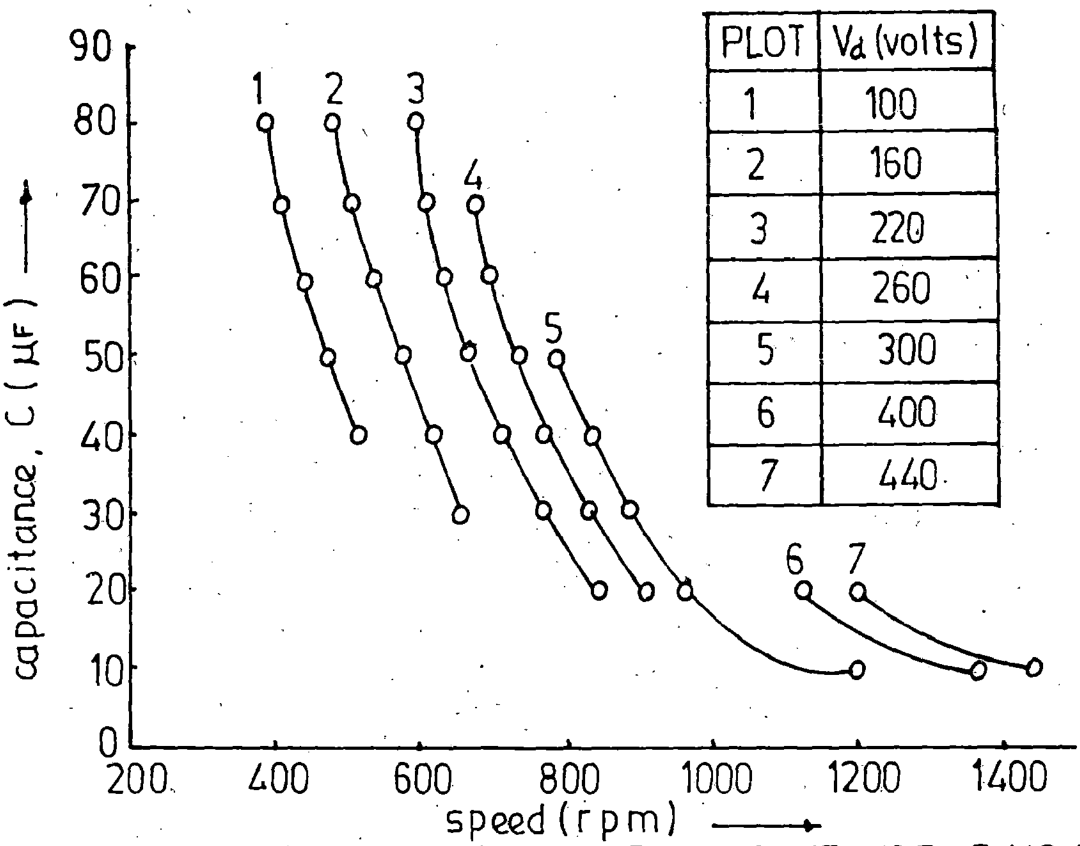

PLOT	V_d (volts)
1	100
2	160
3	220
4	260
5	300
6	400
7	440

FIG.3·3a.VARIATION OF SPEED WITH CAPACITANCE AT NO LOAD.

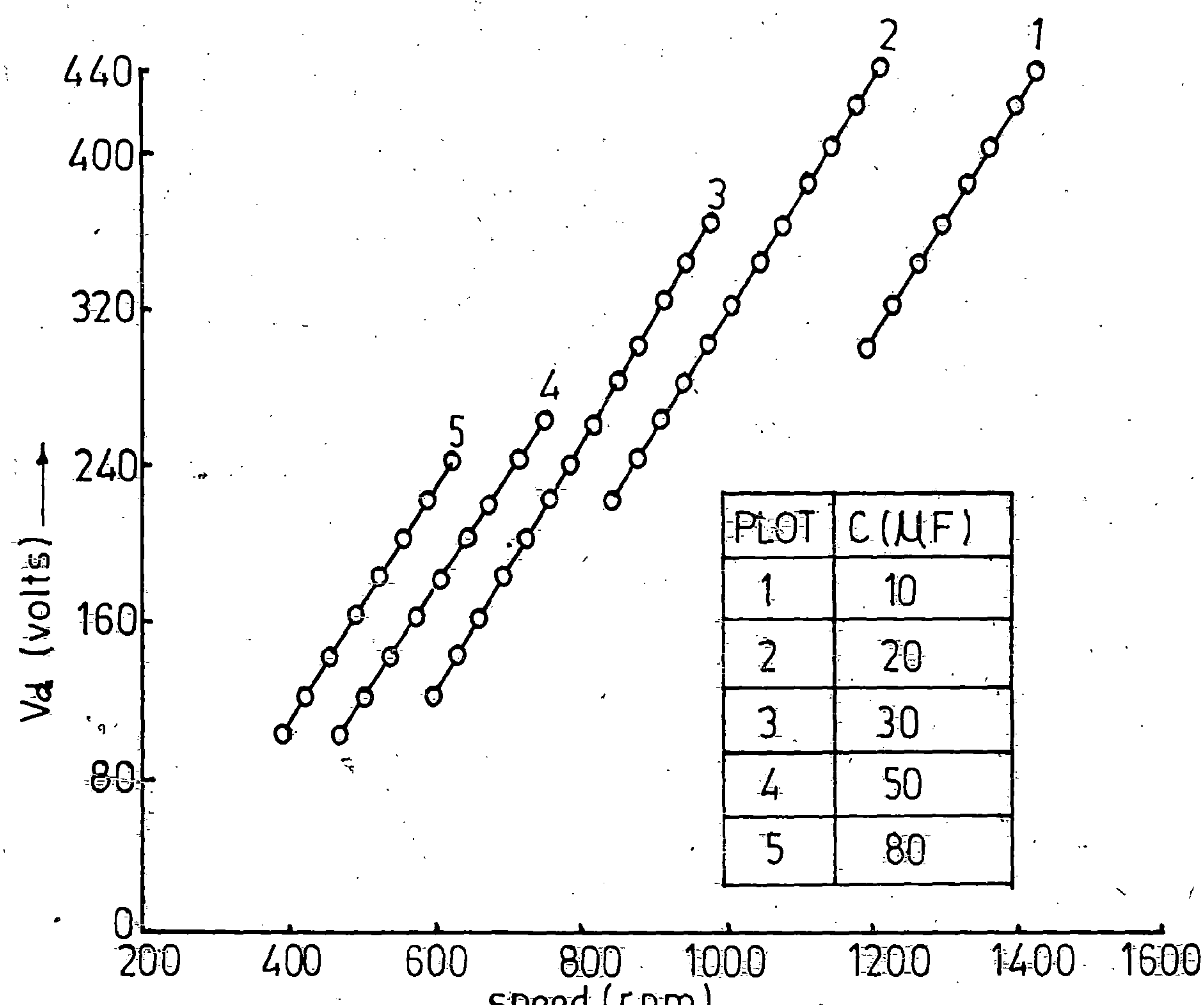

PLOT	C (μF)
1	10
2	20
3	30
4	50
5	80

FIG. 3·3b.VARIATION OF D C LINKVOLTAGE (V_d) WITH SPEED AT NO LOAD.

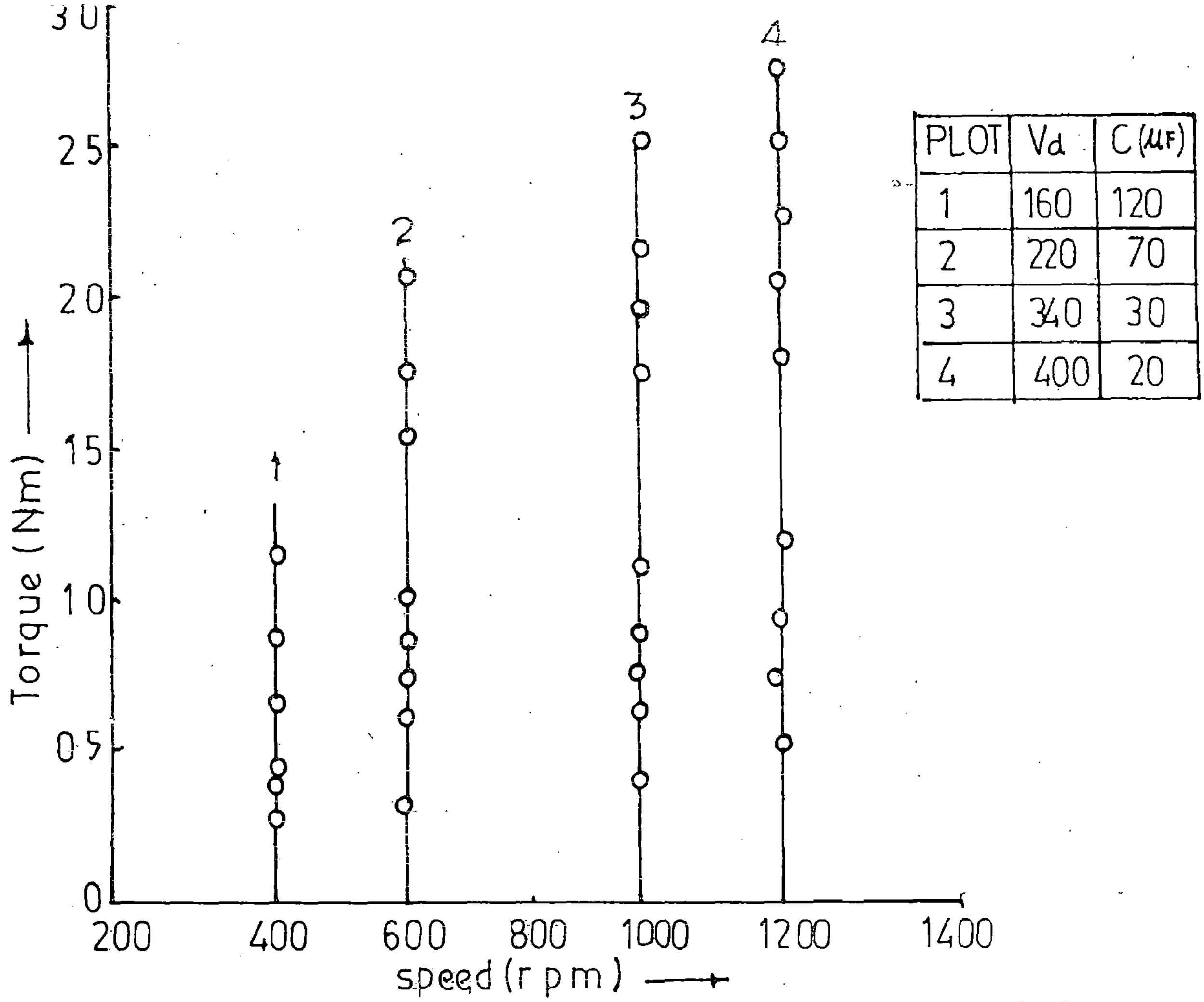

FIG.3·4a. TORQUE-SPEED CHARACTERISTICS OF LCE FED RELUCTANCE MOTOR.

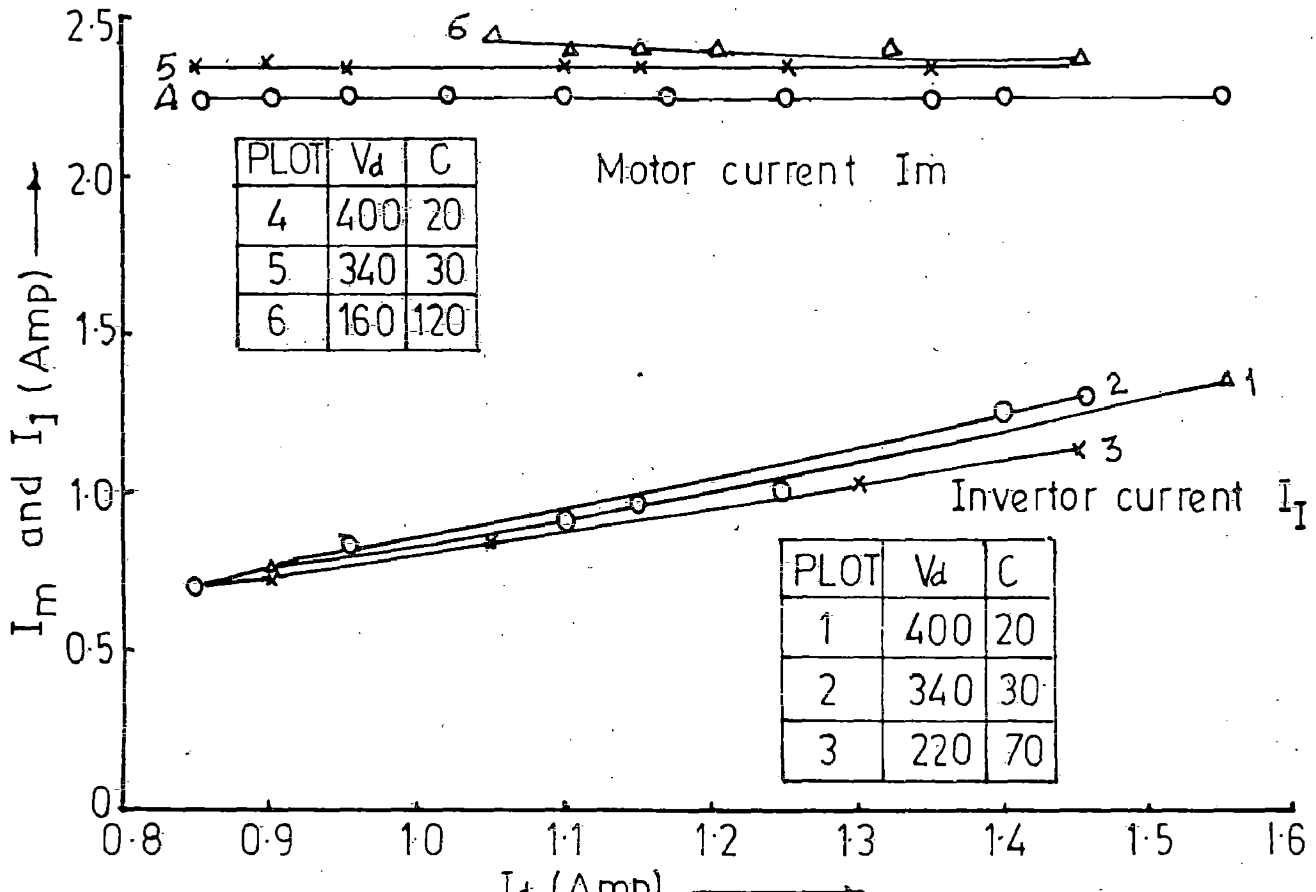

FIG.3·4b. VARIATION OF MOTOR AND INVERTER CURRENT WITH D.C. LINK CURRENT

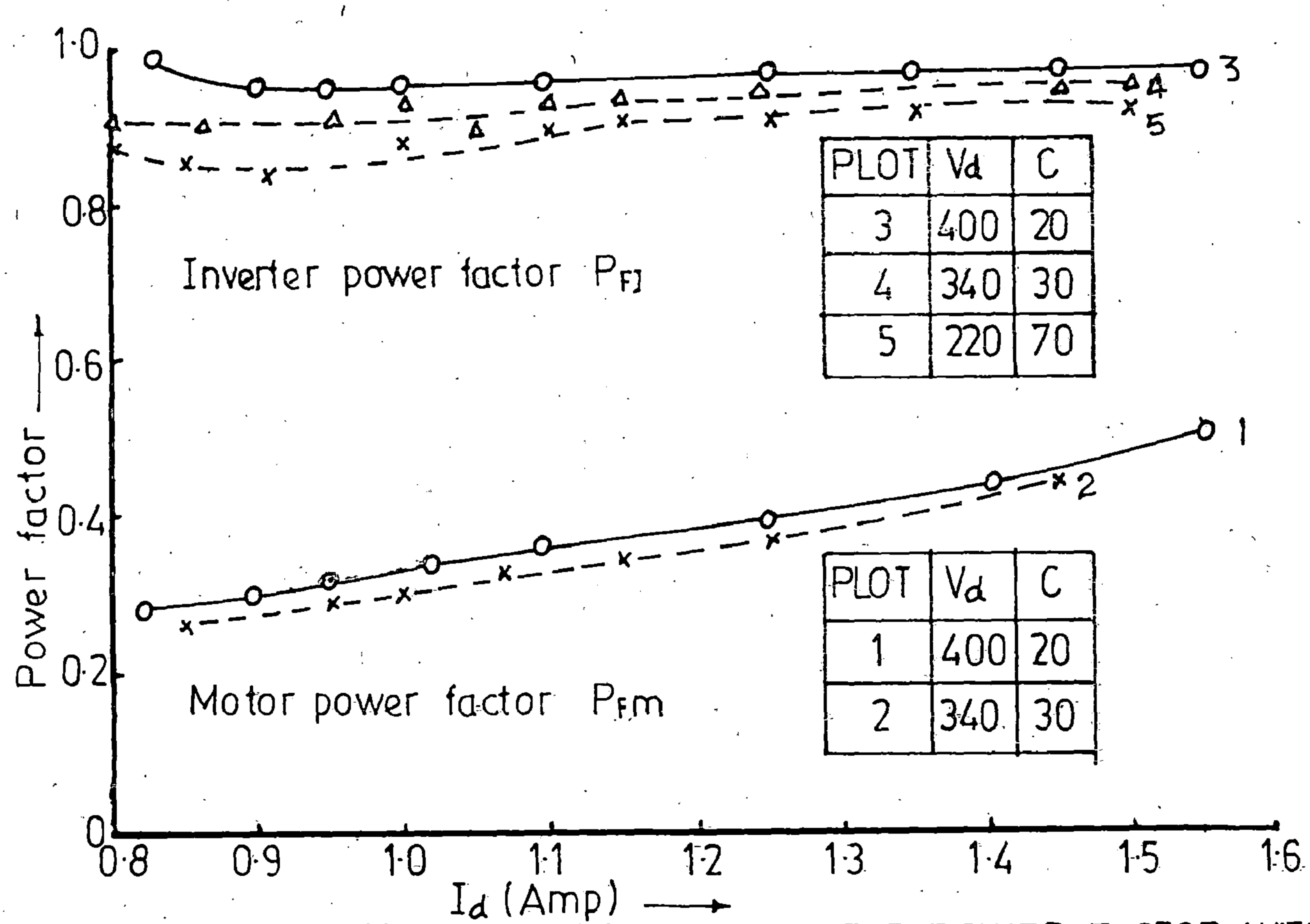

FIG.3·5a. VARIATION OF INVERTOR AND MOTOR POWER FACTOR WITH D.C. LINK CURRENT

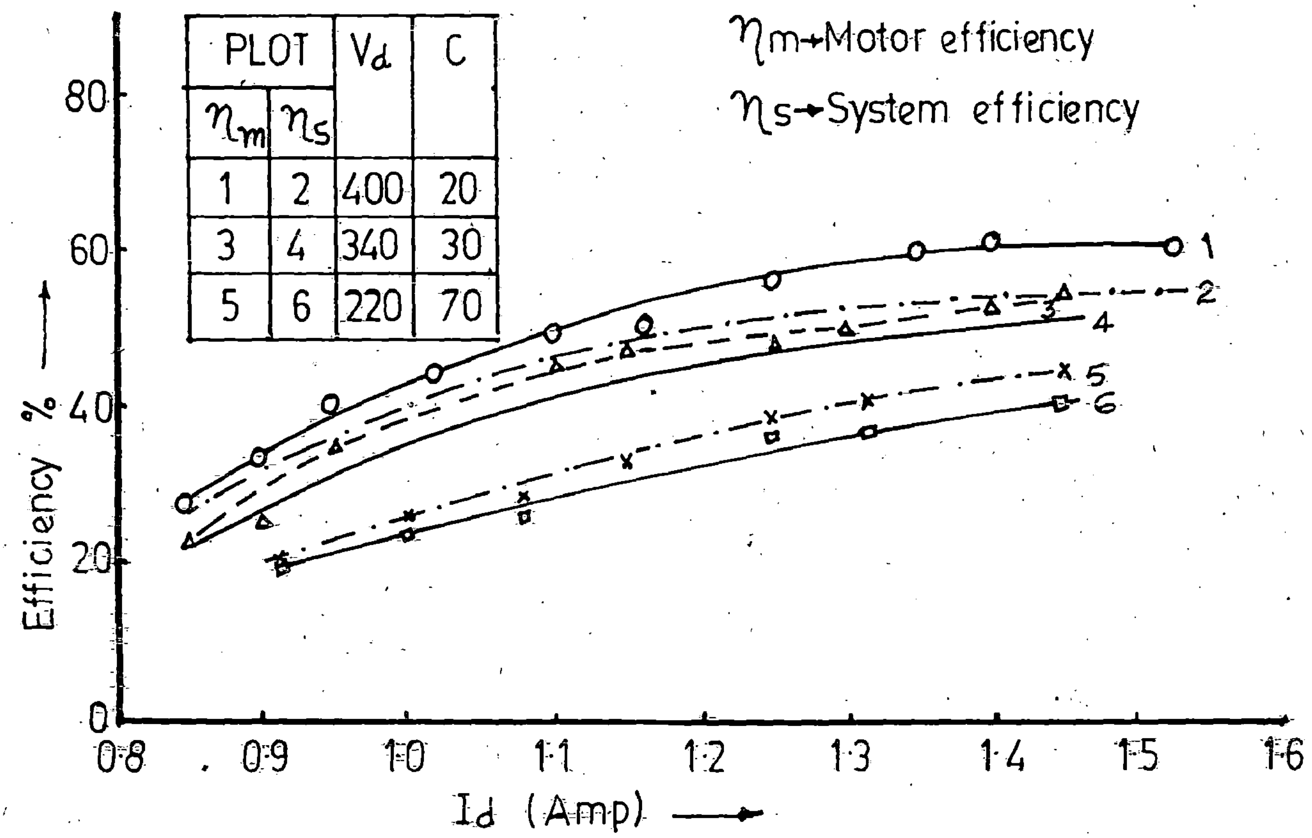

FIG.3·5b. VARIATION OF MOTOR AND SYSTEM EFFICIENCY WITH D C LINK CURRENT.

lower speed output as well as torque limit is also low. On the other hand with high d.c. link voltage and low excitation capacitance resulting the operation in higher speed range. It can, however, be inferred that for most of the purposes, the LCI feed reluctance motor can be treated as constant speed drive.

(iv) Keeping the capacitance and d.c. link voltage fixed it is observed that the motor current remains almost constant or falls slightly as load increases, and the d.c. link current is increased. Fig. 3.4b shows the motor current and inverter current versus the d.c. link current characteristics. The inverter current appears to be increasing linearly with the increase of d.c. link current. It is likely that as the reluctance motor was run under saturated conditions, the variation of load has negligible effect on the motor current. The rates inverter current increase are seen to be almost same for three different conditions and is not dependent upon the operation in particular torque speed range. It will also be clear from the Fig. 3.5a, where inverter power factor characteristics are shown.

(v) The inverter and motor power factor versus d.c. link current curves are shown in Fig. 3.5a. It has been observed that inverter power factor is very high, both at no load and loaded condition and it also does not change appreciably with load. In fact trends show slight increase with increase in load. This is a reason for the inverter current increase linearly with the d.c. link current. The reason for the power factor to be very high (near unity) is that delay angle is close to 180^{0} resulting in little reactive power requirement by the inverter.

The motor power factor is very low at no load and increases linearly with load with different combinatioons if d.c. link voltage and capacitance it was observed that the power factor and its rate of increase are almost identical in all cases.

(vi) The efficiency of the motor and the overall system are shown in Fig. 3.5b. The motor efficiency rises with increased loads on motor. It was also observed that the rate of increase falls at higher loads. The discrepancy of between system and motor efficiency may be attributed due to losses in the inverter and capacitor bank. The rise of efficiency is due to constant losses of the motor from no load to loaded condition caused by constant stator current and constant flux level in the machine. The motor as well as system efficiencies decreases with reduced d.c. link voltage and higher capacitance.

(vii) Fig. 3.6 shows waveforms of the d.c. link voltage and link current for both no load and loaded condition of motor for two different combination of d.c. link voltage and terminal capacitance. It is observed that both the voltage and current contain ripples and therefore not perfect d.c. as desired.

In Fig. 3.7, the oscillograms of the inverter and motor voltage and current waveforms are shown for no load as well as load with the same combination of d.c. link voltage and capacitance. Though the voltage waveforms are found to be almost perfectly sinusoidal and free from harmonics, the inverter current waveforms contain lot of harmonics. Unlike the inverter current waveforms, the motor current waveforms are nearly sinusoidal though contain little harmonics and improves with load. Small notches conforming the sequential commutation of six thyristors may also be observed from the voltage waveforms.

Fig. 3.8 shows the voltage waveform along with capacitor current for no load and loaded condition. The capacitor current appears to be almost sinusoidal having little harmonics. In all the cases it was observed that there is no appreciable change in the waveform pattern from no-load to load.

3.5 Conclusions

The performance of the system has been experimentally studied extensively for both no-load and loaded conditions. The variable frequency (or speed) operation of the motor is quite satisfactory under no load condition and covers from very low (25 percent) to near synchronous (10 percent) speed. Even higher speed range above synchronous may be obtained either by increasing the d.c. link voltage or the

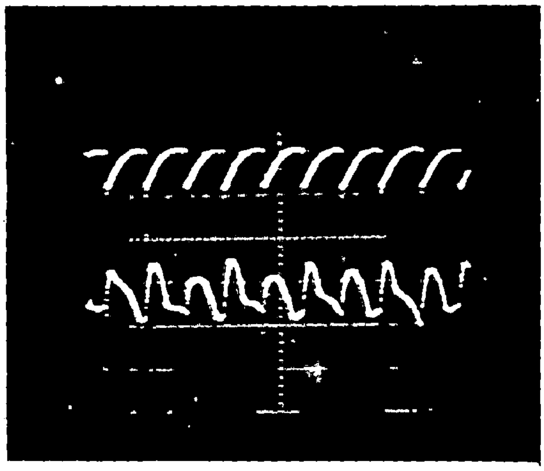

FIG. 3.6(a)

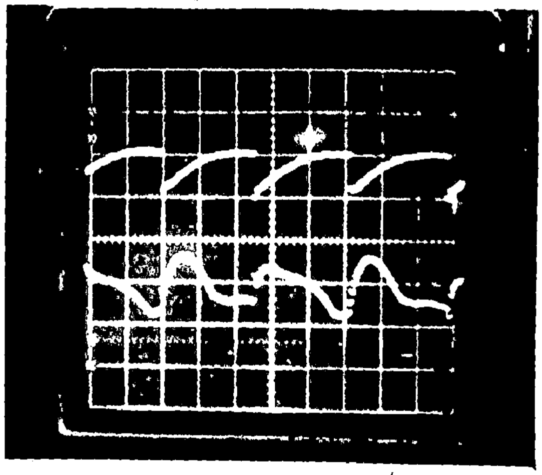

FIG. 3.6(b)

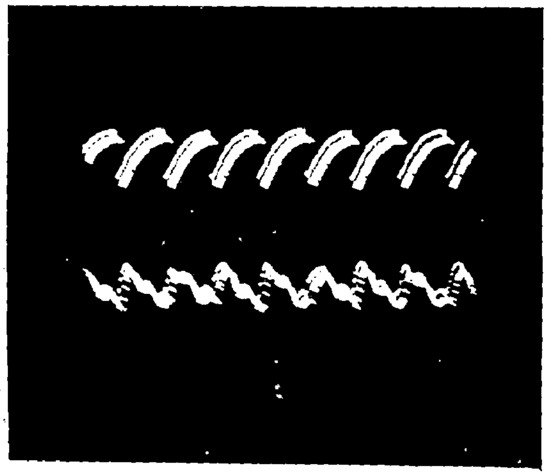

FIG. 3.6(c)

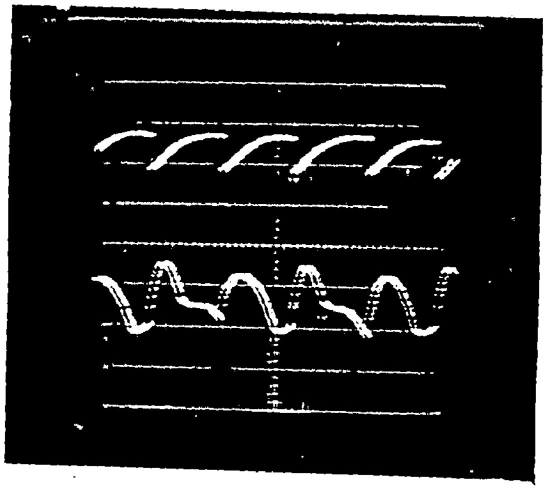

FIG. 3.6(d)

FIG. 3.6 D.C.LINK VOLTAGE AND CURRENT WAVEFORMS

(a) AT NO LOAD (b) AT LOAD (c)= 30uF , V_d= 3 4 0 V)

(c) AT NO LOAD (d) AT LOAD (C= 70 uF, V_d= 220V)

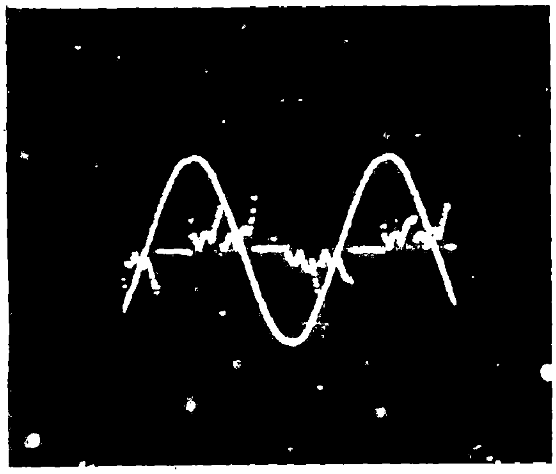

FIG. 3.7a(i)

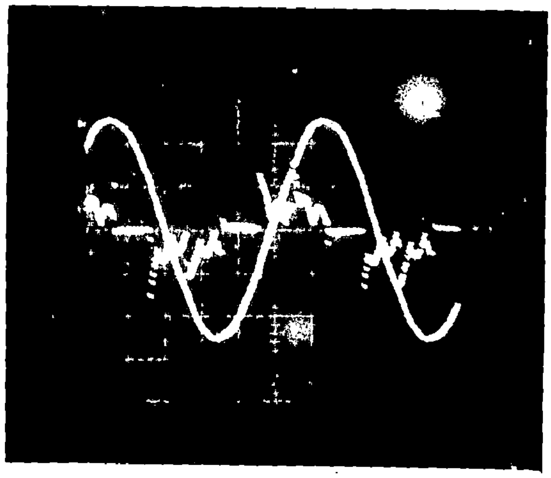

3.7a(ii)

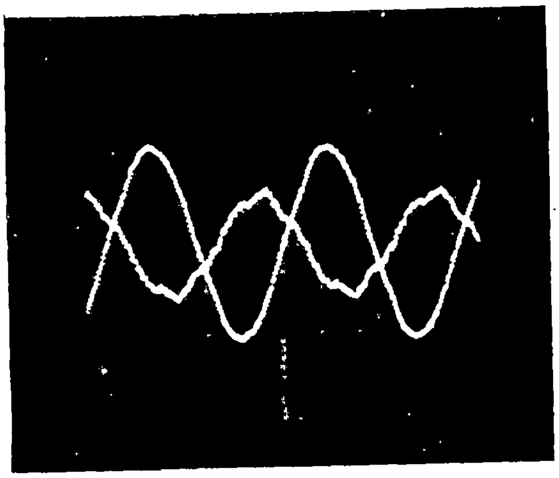

FIG.3.7b(i)

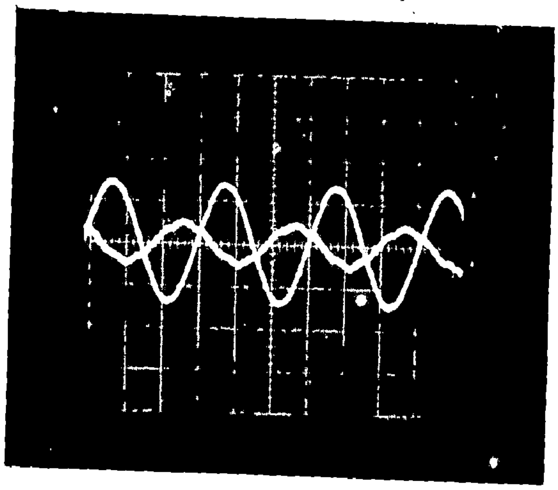

FIG. 3.7b(ii)

FIG. 3.7 VOLTAGE AND CURRENT WAVEFORMS OF (a) INVERTER, (b) MOTOR (i) AT NO LOAD (ii) AT LOAD

(C= 70 uF, V_d = 220V, N = 615 RPM)

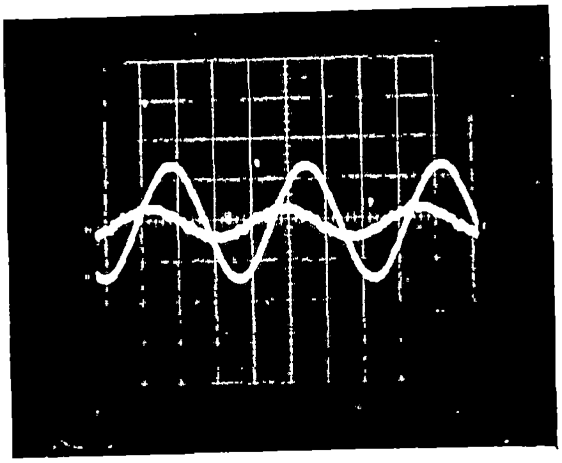

FIG. 3.8a(i)

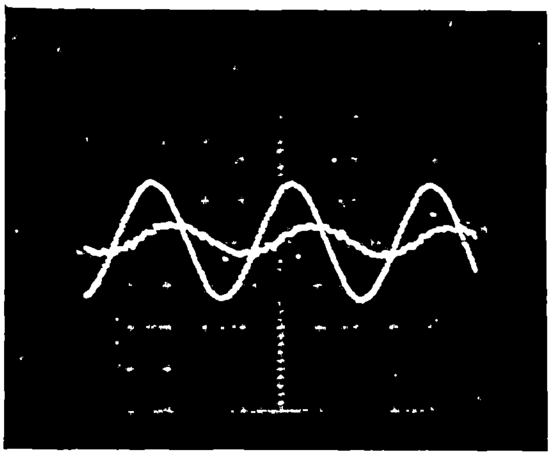

FIG. 3.8a(ii)

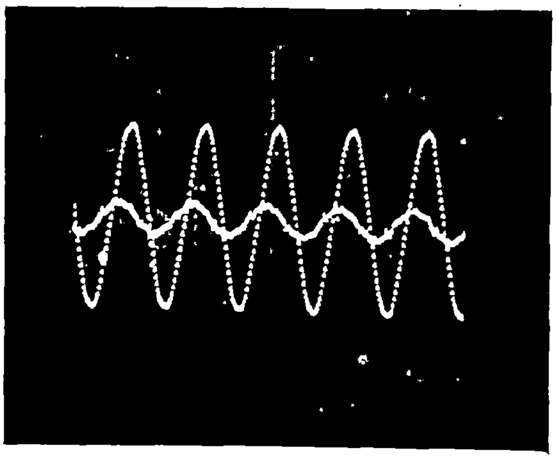

FIG. 3.8(b)

FIG. 3.8 VOLTAGE AND CURRENT OF CAPACITOR

a(i) AT NO LOAD a(ii) AT LOAD (C = 70 uF, V_d = 220 V)

b. AT NO LOAD (C = 30 uF, V_d = 340V)

capacitance. In the loaded condition to get higher torque and the torque-speed characteristics at higher speed range, the d.c. link voltage has to be increased simultaneously decreasing the capacitance. It is very clear that at higher speed range the system is very sensitive to the capacitance. So it is better to vary the capacitance for speed control in higher speed range and the control d.c. link voltage in lower speed range of the proposed drive.

CHAPTER - IV

STEADY STATE ANALYSIS OF THE SYSTEM

4.1 Introduction

The line commutated inverter has now become widely recognised for variable speed ac motor drive. From the experimental investigations of this LCI fed reluctance motor system it is observed that the steady state performance of the system is quite satisfactory. However it is also interesting to observe the analytical performance of the system on the basis of a theoritical model.

Here an effort has been made to develop the steady state analysis of the system. The mode of the system has been developed on the basis of various parameters of the reluctance motor [6-8] and an equivalent circuit approach of the system has been adopted. A generalised model is developed for both no load and loaded conditions of motor. For no load condition the effect of change of the parameter-d.c. link voltage and terminal capacitance, on the variation of speed is studied. For the purpose of comparing the computed results with that from experimentation, wide range of variations of capacitance and d.c. link voltage is considered. In the analysis of loaded condition the suitable combinations of capacitances and d.c. link voltages are taken. A computer algorithm of the analytical expressions is developed and final computation is done with the help of main frame computer. Computed results are plotted alongwith experimental ones to compare and validate developed algorithm.

4.2 ANALYTICAL MODEL

The following simplifying assumptions are taken before developing the model.

(i) The forward drop of thyristors and their losses are neglected.

(ii) The overlap angle is neglected.

(iii) The time and space harmonics are ignored.

(iv) Losses in the capacitor bank are taken to be negligible.

Fig. 4.1 shows the equivalent circuit of the system at any per unit operating frequency F. In this the various expressions are developed in terms of direct and quadrature axis reactances (X_d,X_q) and armature resistance (r_a), of the machine.

For a given d.c. link voltage V_d and inverter firing angle α. The a.c. side inverter voltage per phase V_p may be expressed in the following way

$$V_P = \frac{\pi V_d}{3\sqrt{6}\cos\beta} \qquad \ldots(4.1)$$

where $\beta = (180^{\circ}-\alpha)$ and is known as the inverter angle of advance. In this analysis, for a given value of capacitance C, and d.c. link voltage V_d, the per unit frequency F is the unknown variable to be determined. Subsequently the actual frequency (and also speed) can be found out by multiplying with the base frequency.

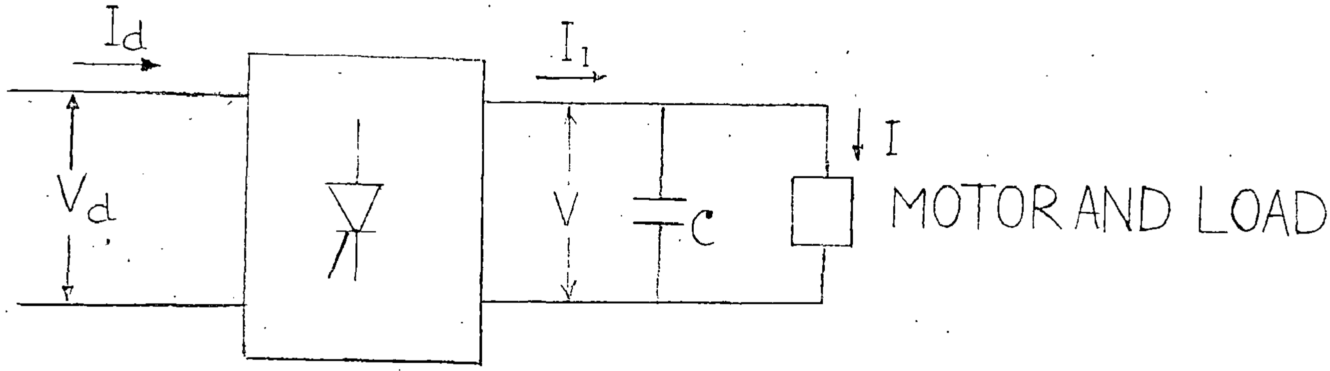

FIG 4.1 EQUIVALENT CIRCUIT OF THE SYSTEM

To obtain an expression for this purpose the active and reactive power balance equations of the whole system are taken. The equivalent circuit of the system is shown in Fig. 4.1.

Active Power Balance

Power supplied by the inverter

$$P_I = VI_1 \cos \beta$$

where, V is the per phase voltage at motor terminals. This is equal to power input to the motor [8].

Therefore,

$$VI_1 \cos \beta = \frac{mV^2}{2(X_d X_q + r_a^2)} \{(X_d - X_q) \sin 2\delta + 2 r_a\} \quad \ldots(4.2)$$

where, m is the number of phases.

δ is the load angle

Reactive Power Balance

Reactive power required by the inverter for its operation

$$Q_1 = VI_1 \sin \beta$$

Reactive power required by the machine and load

$$Q_m = m\, VI \sin \phi$$

where,

ϕ is the power factor angle.

and I is the armature current.

Reactive power supplied by the capacitor $= \dfrac{mV^2 F}{X_C}$

Where X_c is the capacitive reactance at base frequency. Then the reactive power balance equation can be written as

$$\frac{mV^2F}{X_C} = VI_1 \sin\beta + m\, VI \sin\phi$$

or $$VI_1 \sin\beta = \frac{mV^2F}{X_C} - mVI \sin\phi \qquad \ldots(4.3)$$

The power factor of the machine can be given by the expression.

$$\cos\phi = \frac{P_I}{mVI}$$

From this on simplification:

$$mVI \sin\phi = \sqrt{(mVI)^2 - P_I^2}$$

which when substituted in (4-3) gives

$$VI_1 \sin\beta = \frac{mV^2F}{X_C} - \sqrt{(mVI)^2 - P_I^2} \qquad \ldots(4.4)$$

The armature current I can be expressed as

$$I = \frac{V}{X_dX_q + r_a^2}\{(X_q \cos\delta - r_a \sin\delta)^2 + (X_d \sin\delta + r_a \cos\delta)^2\}^{1/2}$$

$$\ldots(4.5)$$

Now using (4.2) and (4.5) equation (4.4) can be written as

$$VI_1 \sin\beta = \frac{mV^2F}{X_c} - \frac{mV^2}{X_dX_q + r_a^2}[(X_q\cos\delta - r_a \sin\delta)^2 +$$

$$+(X_d\sin\delta + r_a \cos\delta)^2 - \tfrac{1}{4}\{(X_d - X_q)\sin 2\delta + 2r_a\}^2]^{1/2}$$

$$\ldots(4.6)$$

Dividing (4.6) by (4.2) and after simplification it becomes as

$$F(X_dX_q+r_a^2) - 0.5X_c \tan\beta(X_d-X_q)\sin 2\delta - X_c r_a \tan\beta$$

$$- X_c[(X_q\cos\delta - r_a\sin\delta)^2 + (X_d\sin\delta + r_a\cos\delta)^2$$

$$- \tfrac{1}{4}\{(X_d-X_q)\sin 2\delta + 2r_a\}^2]^{1/2} = 0 \qquad \ldots(4.7)$$

The load angle δ is related to the power output, P_o in the following way

$$P_o = \frac{mV^2(X_d-X_q)}{2(X_dX_q+r_a^2)^2}\{(X_dX_q-r_a^2)\sin 2\delta + r_a(X_d+X_q)\cos 2\delta$$

$$- r_a(X_d-X_q)\} - P_L \qquad \ldots(4.8)$$

To solve for δ at specified power (P_o) the above equation may be further simplified as

$P_o = A_1\cos 2\delta + A_2\sin 2\delta - A_3$ then it can be written as

$$P_o = A_4\cos 2(\delta_{max} - \delta) - A_3$$

Where δ_{max} is the load angle corresponding maximum output power i.e. pull-out power and may be defined as

$$\delta_{max} = 0.5\tan^{-1}(A_2/A_1) \qquad \ldots(4.9)$$

Then for any output power P_{oR}, the load angle δ_{OR} may be calculated from the expression

$$\delta_{oR} = \delta_{max} - 0.5\cos^{-1}\{(P_{OR} + A_3)/A_4\} \qquad \ldots(4.10)$$

where the parameters A_1, A_2, A_3, A_4 and A_5 are

$$A_1 = A_5(X_d+X_q)r_a$$

$$A_2 = A_5(X_dX_q-r_a^2)$$

$$A_3 = A_5(X_d-X_q)r_a + P_L \qquad \ldots(4.11)$$

$$A_4 = \sqrt{A_1^2 + A_2^2}$$

and

$$A_5 = \frac{mV^2(X_d-X_q)}{2(X_dX_q+r_a^2)^2}$$

For no-load condition $P_{oR}=0$, then $\delta_{oR}=\delta_o$ and can be simplified as

$$\delta_o = \delta_{max} - 0.5\cos^{-1}(A_3/A_4) \qquad \ldots(4.12)$$

Having obtained δ_o in terms of X_d, X_q, r_a, P_L and P_o, it is now evident from equation (4.7) that it contains only unknown variable F alongwith these parameters.

Let some nondimensional parameters be defined as the ratios.

$$K_x = X_d/X_q; \quad K_R = r_a/X_q; \quad K_c = X_c/X_q \qquad \ldots(4.13)$$

Equation (4.7) can be normalised by dividing the entire equation by the factor X_q^2. Having done this and with the help of (4.13), equation (4.7) now becomes

$$F_N(F) = A_{F_1} - A_{F_2} - A_{F_3} - A_{F_4} = 0 \qquad \ldots(4.14)$$

where,

$$A_{F_1} = F(K_x + K_R^2)$$

$$A_{I_2} = K_c[(\cos\delta - K_R\sin\delta)^2 + (K_x\sin\delta + K_R\cos\delta)^2 - \frac{1}{4}\{(K_x-1)\sin 2\delta + 2K_R\}^2]^{1/2}$$

$$A_{F_3} = 0.5\,K_c\tan\beta\,(K_x-1)\sin 2\delta$$

$$A_{F_4} = K_c \cdot K_R\tan\beta$$

The power factor can also be expressed with the help of (4.13).

$$\cos\phi = \frac{(K_x-1)\sin 2\delta + 2K_R}{[2\{(K_x^2-1) + 2K_R(K_x-1)\sin 2\delta - (K_x^2-1)\cos 2\delta + 2(K_R^2+1)\}]^{1/2}} \qquad \ldots(4.15)$$

Before going for the solution of (4.14), the various parameters X_d, X_q, r_a and no load loss of the test machine have to be found out. The armature resistance r_a was measured by easy way. The method, described by Honsinger [6,7], to determine the X_d, X_q parameters and P_L are used here. According to that theory X_d can be measured from no-load test

$$X_d = \sqrt{\left(\frac{V}{I_o}\right)^2 - r_a} \simeq \frac{V}{I_o} \qquad \ldots(4.16)$$

where V is the voltage applied to motor per phase, and I_o is the no load current.

From load test

$Z = \frac{V}{I}$ where I is the motor current when loaded.

Then $R = Z \cos \phi$ and $X = Z \sin \phi$

where ϕ is the power factor of the load

X_q is given by

$$X_q = \frac{X(X_d - X) - (R - r_a)^2}{[1 + g_i(g_i Z^2 - 2R)]X_d - X} \qquad \ldots(4.17)$$

where,

$$g_i = \frac{W_o}{mV^2}$$

and $W_o = P_L - m\, I_o^2\, r_a$

where

P_L = no load losses

The parameters X_d, X_q and P_L are then determined for various supply voltages. The computer program for this calculation is shown in Appendix C_1. The parameters are then plotted as a function of V/F and shown in Fig. 4.2. The characteristics are approximately linearized for simplicity's sake. Then each can be expressed as an equation of straight line.

$$X_d = B_{K_1} - B_{K_2}(V/F)$$
$$X_q = C_{K_1} - C_{K_2}(V/F) \qquad \ldots(4.18)$$
$$P_L = A_{K_1} + A_{K_2}(V/I)$$

4.3 Computation of Performance Characteristics and Their Experimental Verification

It now becomes apparent that with all parameters known, the only unknown variable in equation (4.14) is F, the per unit frequency. The parameters X_d and X_q are frequency dependent quantities. Earlier they were measured at the supply frequency. So now they need to be multiplied by the per unit frequency F. After doing this (4.14) becomes a non-linear algebric equation having polynomial of F. There are several techniques to solve this equation (i.e. solve for F) for certain given values of d.c. link voltage V_d, capacitance C and inverter firing angle α. The approach adopted here is the single variable optimization technique to compute the value of F.

The solution is carried out for both no load and loaded conditions, the optimization technique remaining the same. The no load solution is the simplified form of that with load when simplified δ of (4.12) is used instead of (4.10). The

$V_F \geq 195, \quad P_L = -548.27 + 3.659\, V_F$

$V_F < 195, \quad P_L = -33.6 + 1.05\, V_F$

} $V_F < 100 \; ; \quad P_L = 60$

$V_F \leq 204, \quad X_D = 383.33 - 1.333\, V_F$

$V_F > 204, \quad X_D = 290.77 - 0.923\, V_F$

} $V_F > 270; \quad X_D = 40$

$V_F \leq 200, \quad X_Q = 163.39 - 0.637\, V_F$

$V_F > 200, \quad X_Q = 123.5 - 0.4375 V_F$

} $V_F > 260, \quad X_Q = 10$

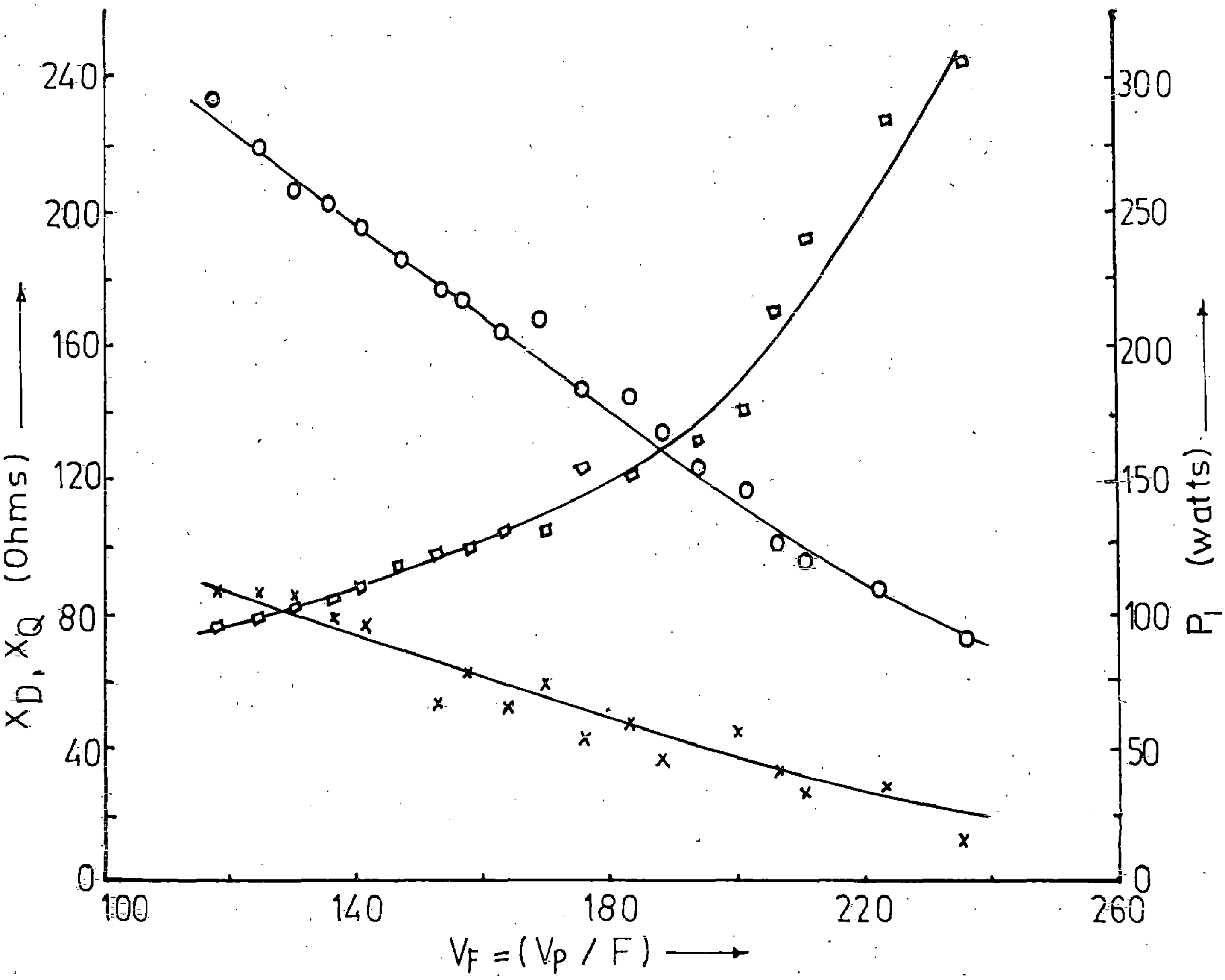

FIG. 4·2. VARIATION OF X_D X_Q AND P_L WITH VOLTAGE AND FREQUENCY

$V_F \geq 195, \quad P_L = -548.27 + 3.659\, V_F$
$V_F < 195, \quad P_L = -33.6 + 1.05\, V_F$
} $V_F < 100 \; ; \quad P_L = 60$

$V_F \leq 204, \quad X_D = 383.33 - 1.333\, V_F$
$V_F > 204, \quad X_D = 290.77 - 0.923\, V_F$
} $V_F > 270; \quad X_D = 40$

$V_F \leq 200, \quad X_Q = 163.39 - 0.637\, V_F$
$V_F > 200, \quad X_Q = 123.5 - 0.4375 V_F$
} $V_F > 260, \quad X_Q = 10$

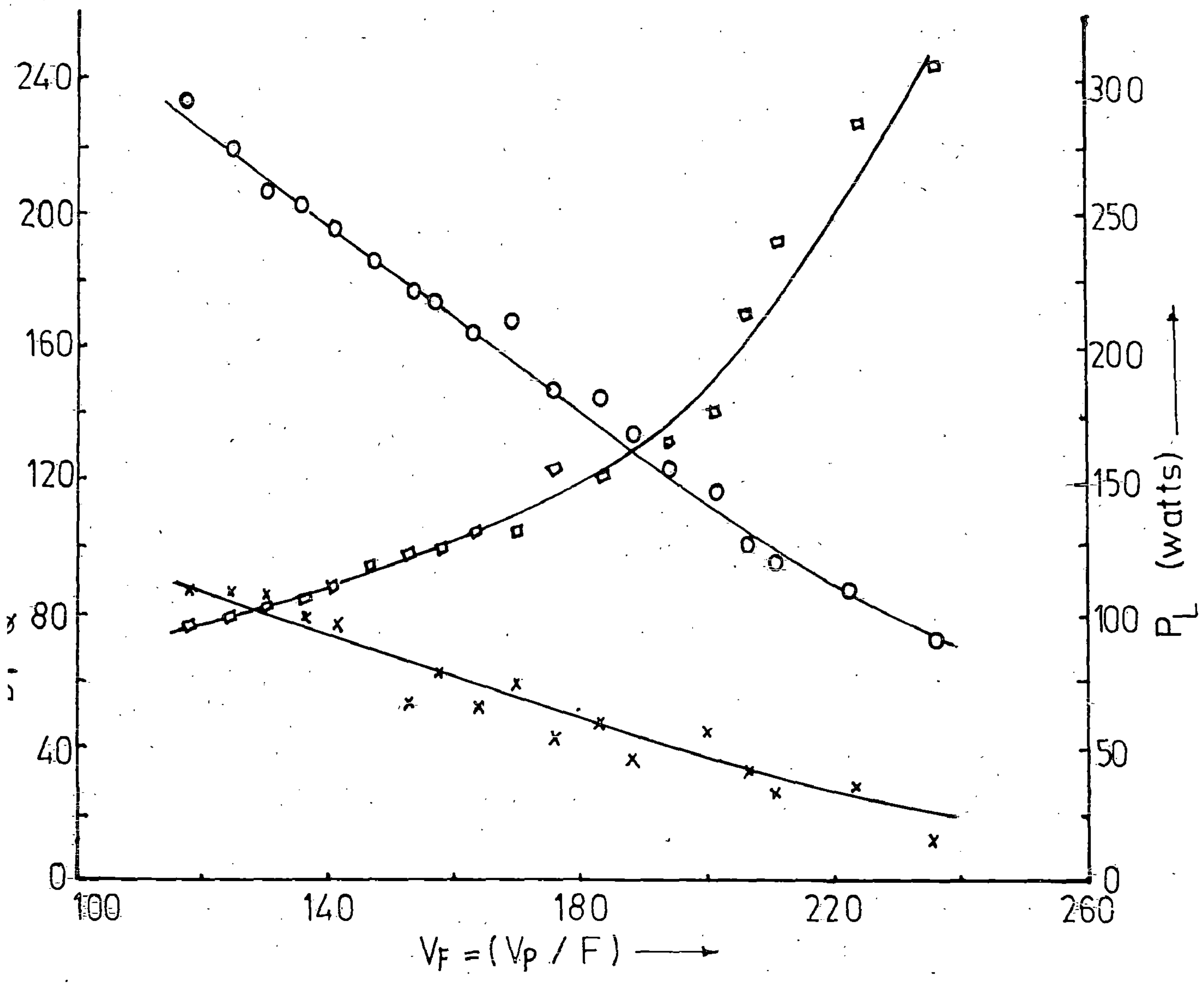

FIG. 4.2. VARIATION OF X_D X_Q AND P_L WITH VOLTAGE AND FREQUENCY

$V_F \geq 195, \quad P_L = -548.27 + 3.659\ V_F$

$V_F < 195, \quad P_L = -33.6 + 1.05\ V_F$

$\} \ V_F < 100 \ ; \quad P_L = 60$

$V_F \leq 204, \quad X_D = 383.33 - 1.333\ V_F$

$V_F > 204, \quad X_D = 290.77 - 0.923\ V_F$

$\} \ V_F > 270; \quad X_D = 40$

$V_F \leq 200, \quad X_Q = 163.39 - 0.637\ V_F$

$V_F > 200, \quad X_Q = 123.5 - 0.4375 V_F$

$\} \ V_F > 260, \quad X_Q = 10$

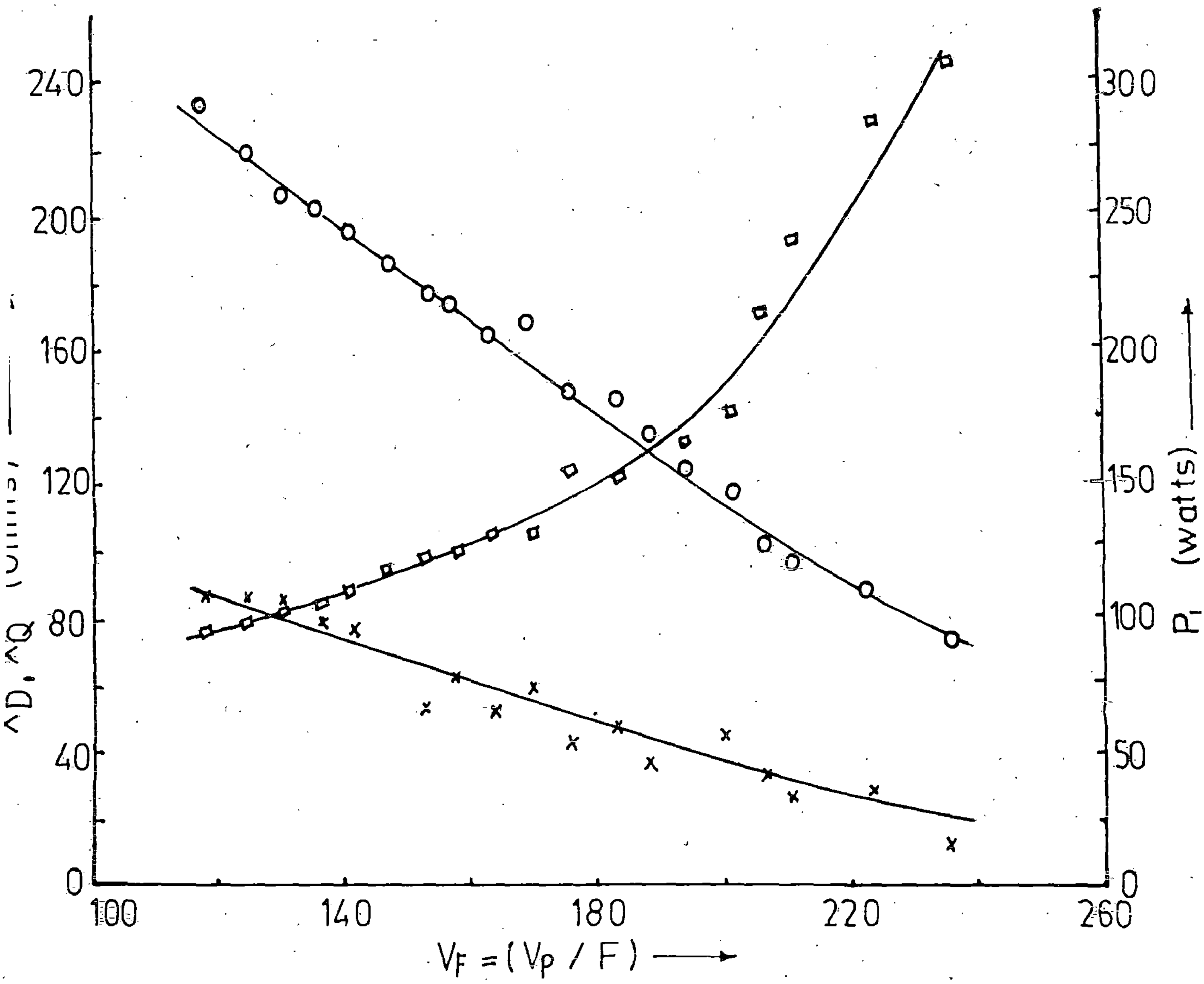

FIG. 4·2. VARIATION OF X_D X_Q AND P_L WITH VOLTAGE AND FREQUENCY method requires an initial guess value of F. Since the solved value of F is to be always positive and usually supposed to be not more than unity, an arbitrary value in this range is taken as the initial guess value. In single variable optimization the whole expression to the left hand side of equation (4.14) (may be called the function) is minimized.

An initial large arbitrary value for the function and suitable step length were chosen. The method is an iterative one. Depending upon whether converging or not after each iteration, the size and direction of the step length is changed.

The iterative process continues till either convergence criterion is satisfied or number of iteration exceeds a predefined number. The flow chart for the developed program is shown in Fig. 4.3, and the developed programs in Appendices C_1 and C_2.

Computation is carried out for no-load and loaded conditions. For no load conditions d.c. link voltage and terminal capacitors are the parameters which are varied to observe their effect on the variation of speed for a wide range. All computational results for no load are plotted in Fig. 4.4. For loaded conditions the computation is carried out for two suitable combinations of d.c. link voltage and terminal capacitor. The different characteristics from the

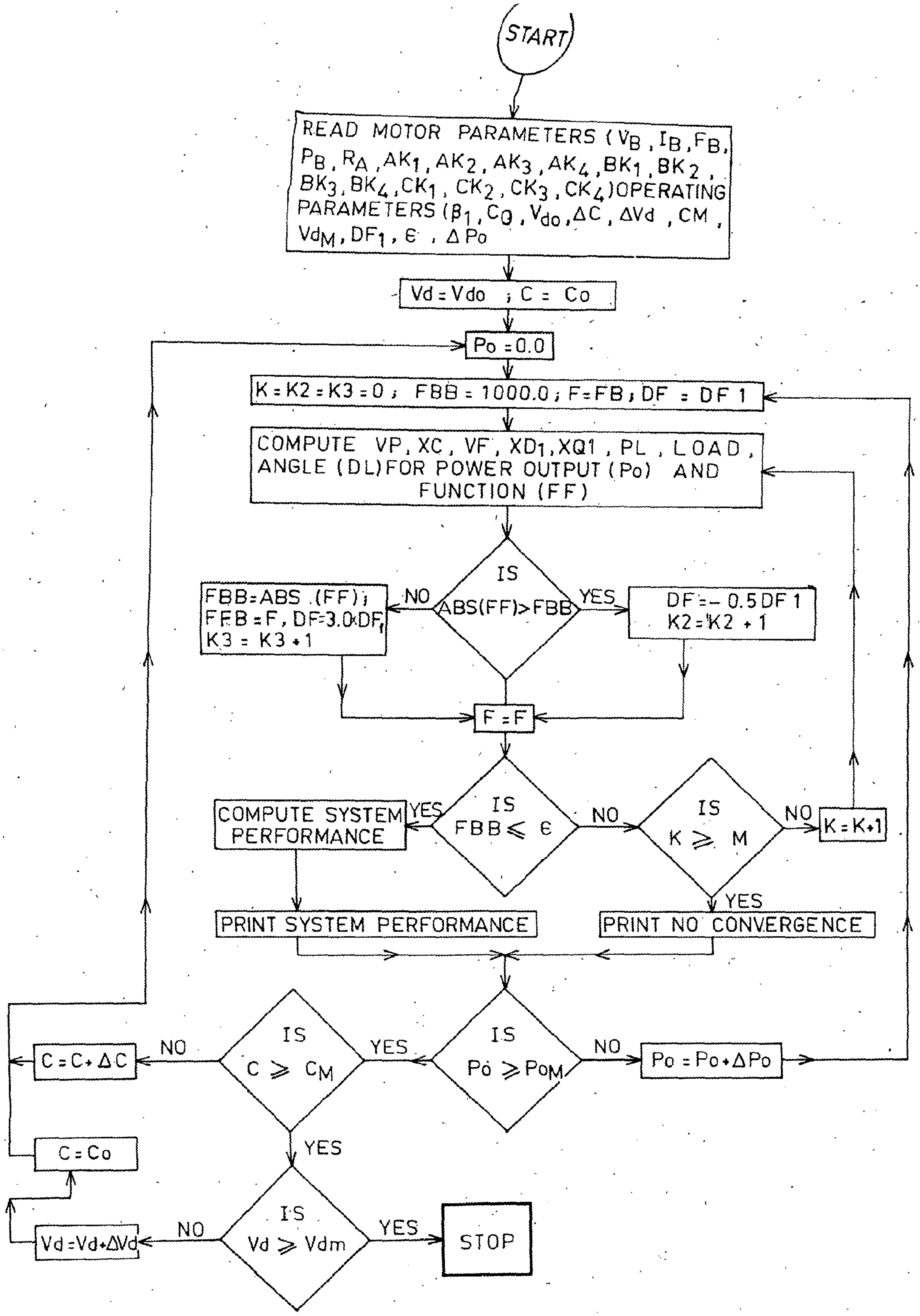

FIG. 43 FLOW-CHART FOR COMPUTATION OF PERFORMANCE OF LINE COMMUTED INVERTER FED RELUCTANCE MOTOR DRIVE.

load test has been plotted in Fig. 4.5 and 4.6. All the computed results are plotted by solid lines.

Experimentation is also carried for the purpose of comparing the computed results with experimental ones. For this purpose, in the no load tests the parameters- d.c. link voltage and capacitor are varied identically as that is done in case of computation. The results from experiments are also plotted in Fig. 4.4 with dotted lines. Tests for loaded condition are carried out with the same combinations of d.c. link voltage and terminal capacitor. For the purpose of comparison the characteristics found from experiments are shown alongwith the computed ones in Fig. 4.5 and 4.6 with test points and dotted lines. In both computation and experimentation the inverter firing angle α is always kept fixed.

4.4 Discussions on Results

The computed results are shown in Fig. 4.4 to 4.6. For both no load and loaded conditions the experimental results are also plotted alongwith the computed one in each case. The following features become evident after comparing these two results.

(i) Fig. 3.4a shows the no load characteristics of speed versus capacitance with d.c. link voltage as the parameter. In all the cases it is observed that the d.c. link voltage has more effect on speed in computed

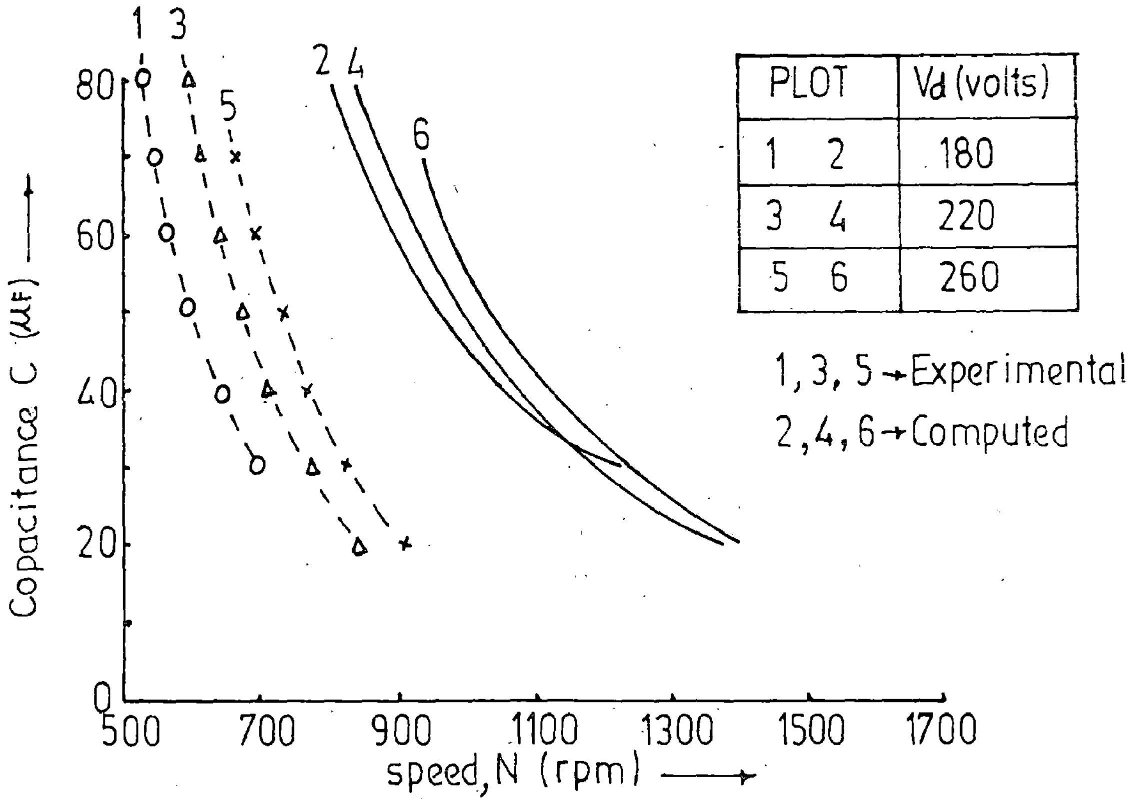

FIG. 4.3a VARIATION OF SPEED WITH CAPACITANCE AT NO LOAD

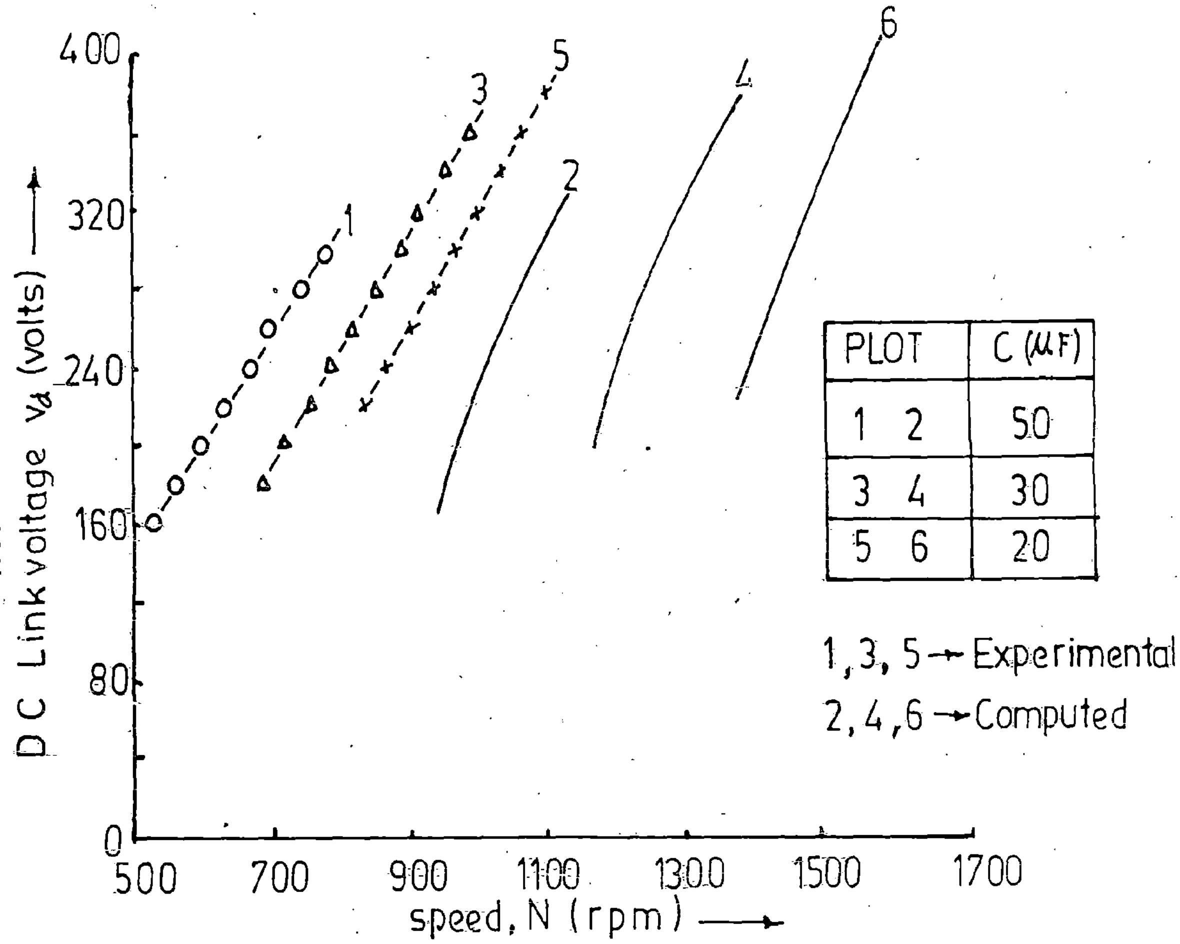

FIG. 4.3b VARIATION OF SPEED WITH D C LINK VOLTAGE AT NO LOAD

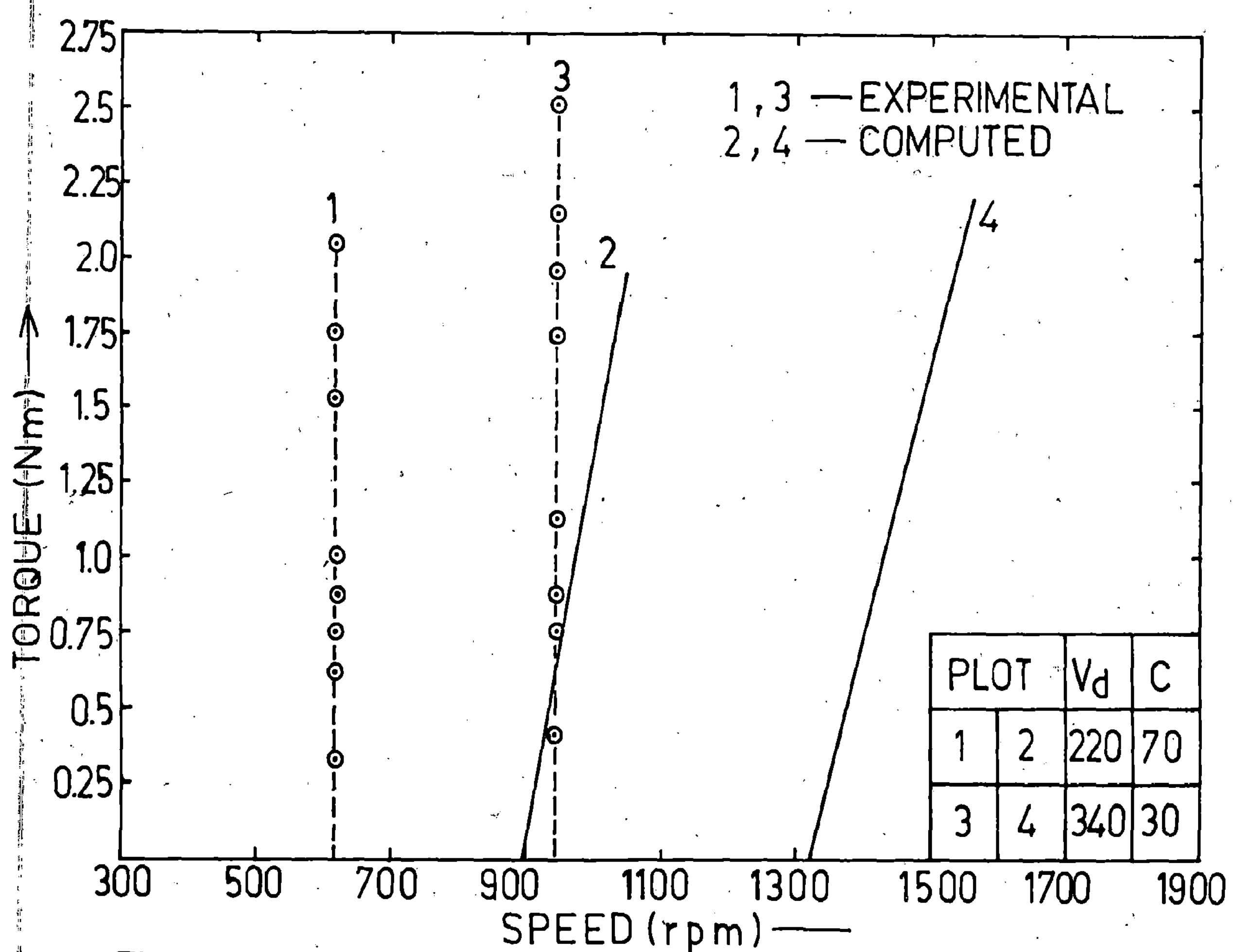

FIG. 4.4(a) TORQUE SPEED CHARACTERISTICS.

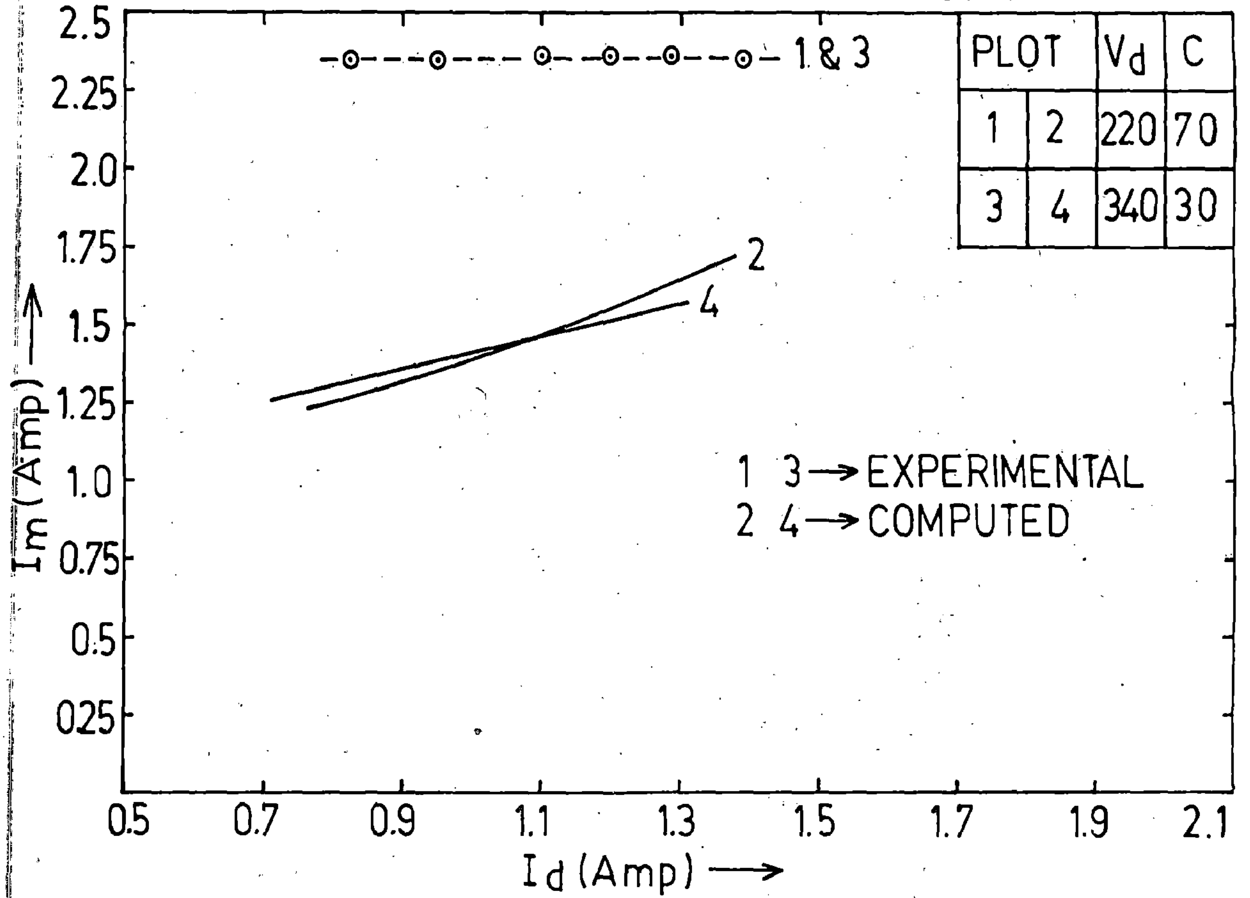

FIG. 4.4(b) VARIATION OF MOTOR CURRENT VERSUS D.C. LINK CURRENT.

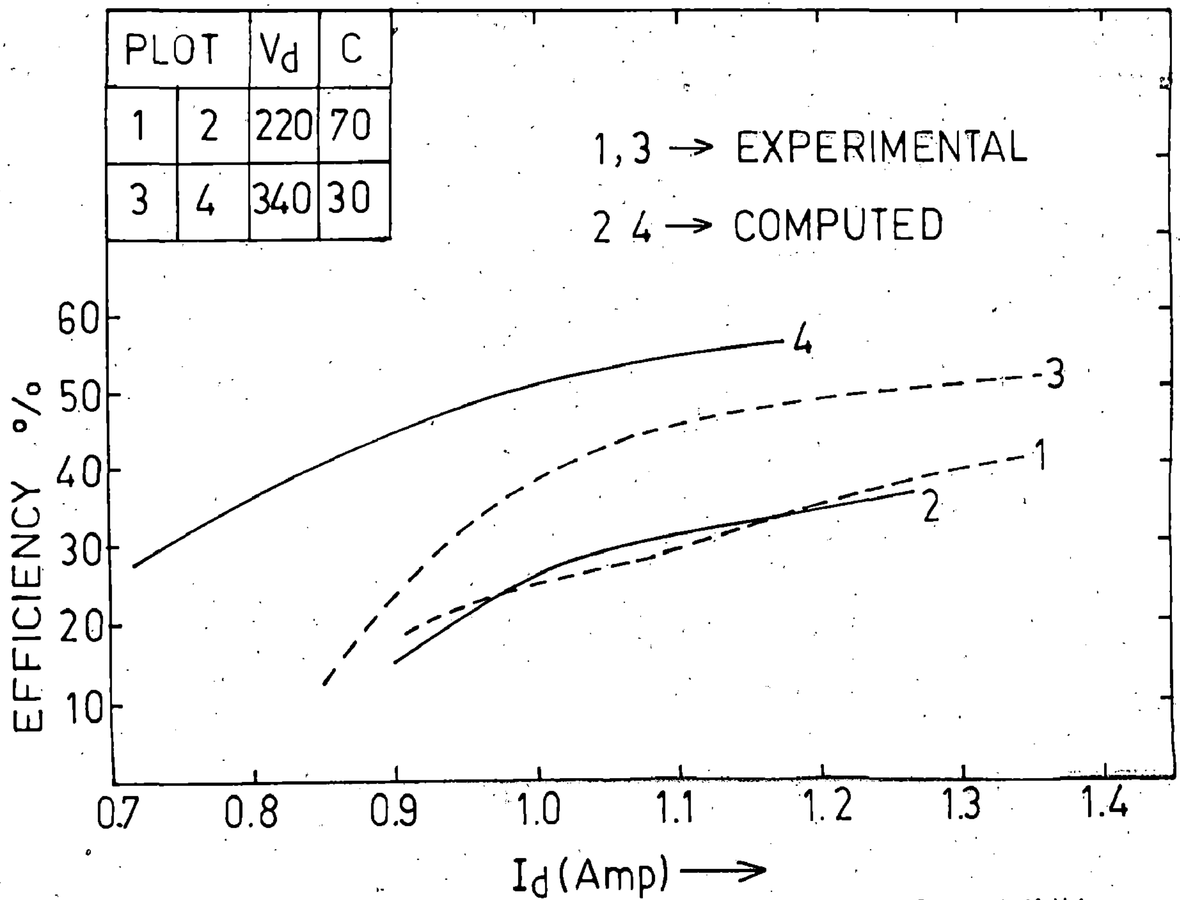

FIG. 4.5 (a) VARIATION OF EFFICIENCY WITH D.C. LINK CURRENT.

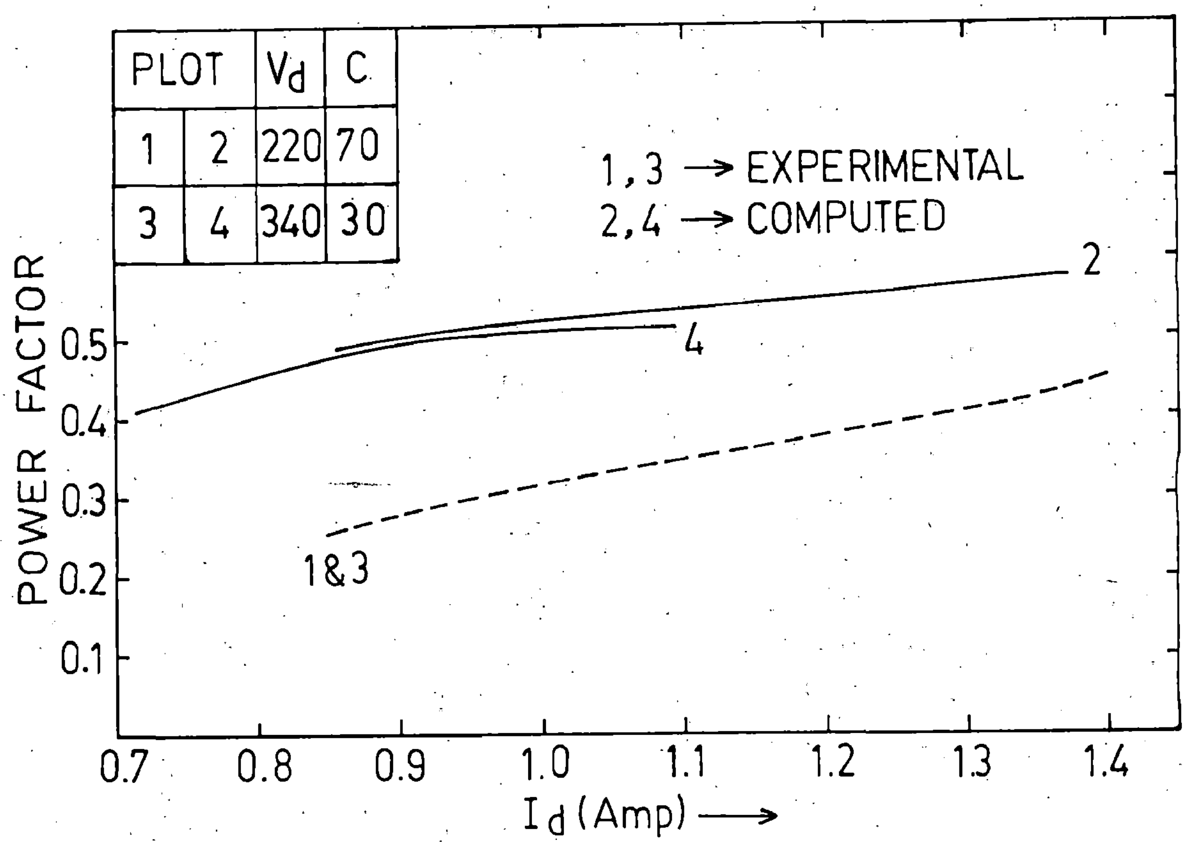

FIG. 4.5 (b) VARIATION OF POWER FACTOR WITH D.C. LINK CURRENT.

results, than in experimental results. Though the patterns of both set of curves is almost same. In lower capacitor ranges the computed speeds are observed to be more sensitive than what they are for experimental results. As a whole it can be said that computed results are differing from experimental results though their pattern remains the same.

(ii) Fig.4.4b shows the variation of speed with the variation of d.c. link voltage for different values of capacitor as the parameter. Here also it is observed that for the same d.c. link voltage higher speeds are obtained from the computed results than that from the experimental ones. Speed is also found to be more sensitive in lower capacitance values as found in earlier case. The patterns of both the experimental and computed curves are identical. The reasons which result in such discrepancy between the experimental and computed results are that the harmonics found in d.c. link voltage and ripples in d.c. link current as well as losses in the inverter are ignored in the development of the model.

(iii) In Fig. 4.5a computed torque speed characteristics under loaded conditions of the motor are shown along with their corresponding experimental ones. The combinations of capacitance and d.c. link voltage are taken for both computation and experimentation. While the experimental results show almost constant speed irrespective of load variations, it is found that the computated speeds are slightly increasing with the increase of torque. The computed characteristics maintains almost linearity as observed in experimental curves.

(iv) For loaded conditions the motor current versus the d.c. link current for two combinations of capacitor and d.c. link voltage are shown in Fig. 4.5b alongwith the corresponding experimental characteristics. The experimental as well as computed motor currents are almost constant with the change of d.c. link current. Though the computed values are at a lower side and the curves show slight increasing trend. The deviations of the computed results from the experimental ones observed in the above cases can be explained by the following reasons.

First, as discussed in first two cases of no load characteristics, the effects of harmonics and losses are ignored. In addition to these, in experimental load tests, the machine was always run under complete saturation and the flux level are maintained for that operation. But the same saturation and flux level are not maintained in the operation of the motor when taken for both computation and experimentation. While the experimental results show almost constant speed irrespective of load variations, it is found that the computated speeds are slightly increasing with the increase of torque. The computed characteristics maintains almost linearity as observed in experimental curves.

(iv) For loaded conditions the motor current versus the d.c. link current for two combinations of capacitor and d.c. link voltage are shown in Fig. 4.5b alongwith the corresponding experimental characteristics. The experimental as well as computed motor currents are almost constant with the change of d.c. link current. Though the computed values are at a lower side and the curves show slight increasing trend. The deviations of the computed results from the experimental ones observed in the above cases can be explained by the following reasons.

First, as discussed in first two cases of no load characteristics, the effects of harmonics and losses are ignored. In addition to these, in experimental load tests, the machine was always run under complete saturation and the flux level are maintained for that operation. But the same saturation and flux level are not maintained in the operation of the motor when computation was done. Extra effect of stray load and other losses may come into picture due to this reason. The ultimate effect of all this factors might have caused such discrepancy between experimental and computed results.

(v) The efficiencies versus d.c. link current are shown in Fig. 3.6a under load condition. Both computed and experimental results are shown. They are found to be very close and the trends of the curves are almost same i.e. with increase in d.c. link current efficiencies are found to be increasing.

(vi) The motor power factor versus d.c. link current are shown in Fig. 3.6b. The power factor, in computed results, are found to be higher than what observed in experiments. But the trends in both the cases are almost same i.e. they are increasing linearly with d.c. link current.

4.5 Conclusions

A complete study of the performance of the LCI-reluctance motor system has been made on the basis of analytical model. Systematic and advanced approach has been taken to develop the theory of the analysis. In the developed technique for the no load and loaded conditions of the motor exact equivalent circuit of the system has been considered. Algorithm and computer program was developed on the basis of single variable optimization technique and the method is found suitable to compute the no load and load performance in terms of speed, torque, efficiency, power factor and currents for different values of d.c. link voltage and terminal capacitance. The computed results are then compared with the experimental ones and they are found to be almost identical. The developed analytical technique and computer program require less computation time and require small memory space of the computer. Therefore, it can be concluded on the basis of experimental and computed results that the performance of LCI fed reluctance motor system is quite satisfactory.

CHAPTER - V

CONCLUSIONS AND SUGGESTIONS FOR FURTHER WORK

5.1 Main Conclusions

Feeling the necessity to explore the feasibility and potentiality of variable speed reluctance motor drive to be realised using line commutated inverter, this investigation was undertaken. In order to achieve the objective the whole scheme was designed, fabricated and tested. The performance of motor with this system is then investigated experimentally for wide range of speed control. An analytical model of the system has been developed in terms of machine parameters. The performance of the system has been computed using the developed model and single variable optimization for different values terminal capacitor and d.c. Link voltage at no load as well as loaded conditions of motor. From the computed results and test results the following conclusions on this investigation may be summarised as follows.

(i) The developed firing circuit and power circuit of the scheme have been found satisfactory to achieve desired operation. The recorded waveforms at different points of the circuit have been observed identical with theoritical ones.

(ii) From the experimental investigations it is observed that the system operates very stably at no load as well as loaded conditions of the motor.

(iii) From the results obtained it is concluded that wide range of speed variation can be achieved for no load and loaded conditions of motor by varying the d.c. link voltage and terminal capacitor.

(iv) An interesting feature of the system has been observed that the speed remains remains almost constant irrespective of load variations and thus it results the constant flux operation over wide speed range at different loads.

(v) The computed results at no load and loaded conditions of motor resembles with the corresponding experimental ones, which confirms the validity of the developed analytical approach.

The system is cheap and simple variable speed drive and therefore supposed to be suitable for various applications. So it can be concluded that a very efficient scheme for variable speed reluctance motor drive has been developed which has sufficient capability and points to a new horizontal of potentiality in the field of drives for industrial applications.

5.2 Suggestions For Further Work

Although the basic objective of dissertation has been fulfilled satisfactorily, the term 'end' never exists in research work, particularly in the field of technology. Certain problems and limitations are observed during the course of investigations which necessitate that further investigations with same or different line of approach can be done for further enhancement. In the light of this the following proposals regarding scope of further work are listed below.

(i) The system is not self-starting for any desired speed. Hence it is very important to develop suitable starting technique to be incorporated with the system so that the system can be started and run at any desired frequency.

(ii) To solve the developed analytical model different numerical approach may be adopted. Accurate model may be developed by taking into account the factors which are neglected here.

(iii) More care and effort can be taken to eliminate the the harmonics and ripples found in d.c. link voltage and current respectively.

(iv) The work has been done on the system in open loop manner. However, for fast response and better controllability and stability, the closed loop incorporating both speed control and current control can be designed for this LCI system.

(v) Only steady -state stability has been investigated. Therefore, the area of studying the transient and dynamic conditions of operations need to be attempted.

(vi) In the present system, analog control scheme has been used. A microprocessor based control technique may be attempted for improvement of system performance in terms of flexibility and ease of operation and faster response.

incorporating both speed control and current control can be designed for this LCI system.

(v) Only steady -state stability has been investigated. Therefore, the area of studying the transient and dynamic conditions of operations need to be attempted.

(vi) In the present system, analog control scheme has been used. A microprocessor based control technique may be attempted for improvement of system performance in terms of flexibility and ease of operation and faster response.

BIBLIOGRAPHY

1. Katsumi Uezato, 'Characteristics of Solid Rotor Three Phase Reluctance Motors', Electrical Engineering in Japan, Vol. 98B, No.9, September 1978, PP.741-748.

2. P.J.Lawrension and L.A.Agu, 'Theory and Performance of Polyphase Reluctance Machines', Proc. IEE , Vol.111, No.8, August 1964, pp.

3. Mahmood H.Nagrial and P.J.Lawrension, 'Optimum Steady-State and Transient Performance of Reluctance Motors', Proc. International Conf. on Electrical Machines, 1984, (Switzerland), Vol.1, PP.321-324.

4. P.J.Lawrension and S.K.Gupta, 'Developments in the Performance and Theory of Segmental-Rotors Reluctance Motors,' Proc. IEE , Vol.114, May 1967, PP.845.

5. A.L.Mohamadien, S.A.Hasan and A.M.F.Osheiba, 'Cageless Reluctance Motor: A New Improvement in Design', Electric Machine and Electromechanics, Vol. 6, No.6, Nov./Dec. 1981, PP. 493-509.

6. Vernon B.Honsinger, 'The Inductance L_d and L_q of Reluctance Machine', IEEE Trans. on PAS, Vol. PAS-90, No.1, Jan/Feb. 1971, PP. 298-304.

7. Vernon B.Honsinger, 'Steady-State Performance of Reluctance Machines', IEEE Trans. on PAS, Vol.PAS-90, No.1, Jan/Feb. 1971, PP. 305-311.

8. K.Vezato and M.Veda, 'Effect of Parameter changes on the Performance of Solid-Rot Three Phase Reluctance Motors', Electric Machines and Power Systems, Vol.8, 1983, PP. 185-197.

9. R.S.Ramshaw, 'Power Electronics Thyristor Controlled Power for electric motor', LONDON CHAPMAN AND HALL

10. J.M.D.Murphy, 'Thyristor Control of A.C.Motors', Pergamon Press, Oxford 1913.

11. G.K.Dubey et.al., 'Thyristorised Power Controllers', Willey Eastern Limited, 1986.

12. B.R.Pelly, 'Thyristor Phase Controlled Converters and Cycloconverters', Willey Inter Science, New York, 1976.

13. B.D.Bedford and R.G.Hoft, 'Principle of Inverter Circuit, Willey, New York, 1969.

14. F.F.Mazda, 'Thyristor Control, Newmens - Butterworths.

15. M.Ramomoorthy, 'An Introduction to Thyristors and Their Applications', East-West Press.

16. B.K.Bose, 'Power Electronics and A.C.Drives', Prentice Hall, New Jersey, 1986.

17. Kenneth F.Phillips, 'Current-Source Converter for A.C. Motor Drives', IEEE Trans. on IA, Vol. IA-8, No.6, Nov.-Dec.,1978, PP. 679-683.

18. G.K.Slemon, Shashi B.Dewan, and J.W.A.Wilson, 'Synchronous Motor Drives with Current-Source Inverter', IEEE Trans. on IA, Vol. IA-10, No.3, May-June 1974, PP. 412.

19. P.C.Sen, 'Thyristor D.C.Drives,'Willey Inter Science, New York - 1981.

20. R.Venkataraman and B.Ramaswami, 'Thyristor Converter Fed Synchronous Motor Drive,' Electric Machine and Electromechanics, Vol. 6, No.5, Sept.-Oct.1981, pp. 433-449.

21. A.C.Williamson, N.A.H.Issa and A.R.A.M.Makky, 'Variable Speed Inverter Fed Synchronous Motor Employing Natural Commutation', Proc. IEE, Vol.125, No.2, March 1978, pp. 113-119.

22. E.P.Cornell and D.W.Novotny, 'Commutation by Armature Induced Voltage', IEEE Trans. PAS, Vol.74, Jan/Feb.1974, pp. 760-766.

23. Hoang Le-Huy, Alain Jakbowicz and R.Perret, 'A Self-Controlled Synchronous Motor Drives Using Terminal Voltage Sensing', IEEE IAS Conf. Rec. 1980, pp. 562-569.

24. Jacques Davoine, R.Perret and H.Le-Huy, 'Operation of a Self-Controlled Synchronous Motor without a shaft position Sensor', IEEE Trans. on IA, Vol.IA-19, No.2, March/April, 1983.

25. M.V.S.S.Ranganadhachari, B.P.Singh, R.Anbarsu and R.Arockiasamy, 'Experimental Investigations' on Steady-State Performance of Commutator-less Machine Induction Motor System', Institute of Engineers (I), Vol.64, Pt. EL3, Dec. 1983.

26. M.V.S.S.Ranganadhachari, B.P.Singh, R.Anbarsu and R.Arockiasamy, 'Experimental Investigations on Line Commutated Invertor-Synchronous Machine as a Variable Frequency Source', Electric Machine and Power System, 9: 13-21, 1984.

27. Ajay Kumar, R.Anbarasu and B.P.Singh, 'Steady State Performance of Series Commutatorless DC Motor', JIE (India), Vol.65, No. Pt. EL, No.6, June 1985, pp.185-188.

28. C.Namuduri and Paresh.C.Sen, 'Digital Simulation of an Inverter-Fed Self-Controlled Synchronous Motor', IEEE Trans. on Industrial Electronics, Vol. IE-34, No.2, May 1987, pp. 205-215.

29. John. Rosa, 'Utilization and Rating of Machine Commuted Invertor Synchronous Motor Drive', IEEE Trans. on IA, Vol. IA-15, No.2, March/April 1979.

30. Teruo Kotaoka and Shoh Nishikata,'Transient Performance Analysis of Self-Controlled Synchronous Motors', IEEE Trans on -IA, Vol.IA-17, No.2, March/April 1981.

31. D.B.Watson, 'Induction Motor Drive from Self-Commutating Inverter', IEE Proc., Vol. 128, Part B, No.1, Jan. 1981.

32. D.B.Watson, 'Performance of Induction Motor Driven from Self-Commutating Inverter,' IEEE Proc., Vol.129, Part B, No.5, Sept. 1982, pp. 248-250.

33. Bhim Singh, K.B.Naik and A.K.Goel, 'Experimental Investigation of Steady-State Performance of a Self-Commitated Inverter Fed Induction Motor System.', The Institution of Engineers (India), Vol. 68, Part EL2, Oct. 1987, pp. 41-45.

34. Sejin Seong and Tadashi Fukao, 'An Analysis and Characteristics of A new High Frequency Drive Induction motor system', IEEE/IAS 83 Annual Meeting, pp. 580-587.

35. A.R.Stocken, 'Synchronous Motor, Variable Speed A.C.Drives System,' Conference Publication No.179 IEE, Conference on Variable Speed Drives, 25-27, Sept. 1979, pp. 58-60.

36. Bimal K.Bose, 'Adjustable Speed A.C.Drives-A Technology Status Review', Proc. IEEE, Vol.70, No.2, February 1982, pp. 116-135.

37. B.L.Jones and J.E.Brown, 'Electrical Variable-Speed Drives', An IEE Review Proc. IEE, Vol.131, Pt.A, No.7, September 1984, pp. 516-558.

38. S.S.Rao, 'OPTIMIZATION-Theory and Applications', Willey Eastern Limited.

APPENDIX – A

PIN DETAIL AND CONNECTION DIAGRAM OF DIFFERENT ICs.

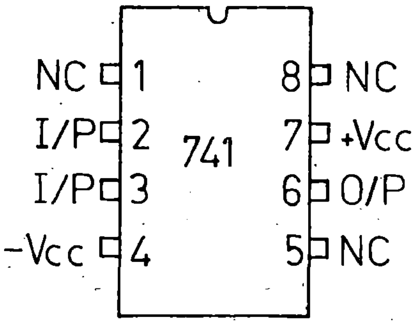

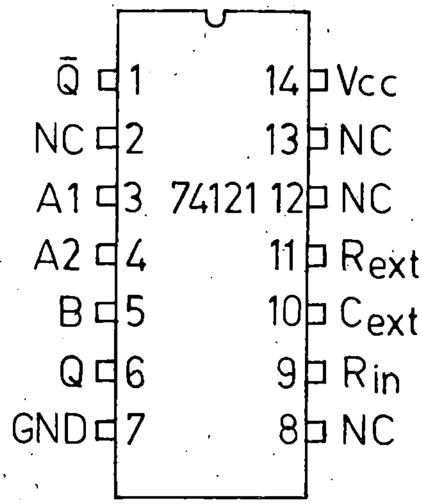

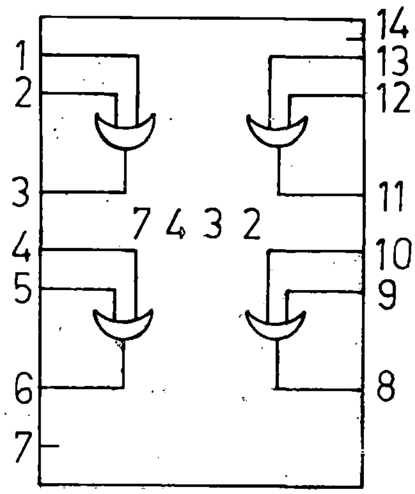

TRUTH TABLE FOR IC-74121

INPUTS			OUTPUTS	
A_1	A_2	B	Q	$\bar{Q}$
L	X	H	L	H
X	L	H	L	H
X	X	L	L	H
H	H	X	L	H
H	↓	H	⊓	⊔
↓	H	H	⊓	⊔
↓	↓	H	⊓	⊔
L	X	↑	⊓	⊔
X	L	↑	⊓	⊔

H ⟶ HIGH LEVEL

L ⟶ LOW LEVEL

X ⟶ DON'T CARE

↑ ⟶ TRANSITION FROM LOW TO HIGH LEVEL

↓ ⟶ TRANSITION FROM HIGH TO LOW LEVEL

APPENDIX - B

DETAILS AND PARAMETERS OF THE MACHINE USED

1. Detail Ratings of the Machines

   (i) Reluctance Motor: 0.5 KW, 230V, 2.5A
   Star Connected, 4 pole, 50 Hz, 50 Hz.

   (ii) D.C.Machine coupled to the R.M: 1.0 H.P., 220/30 V, 4.6A, 1450 xpm.

2. Parameters of Machine

   Armature resistance per phase of the reluctance motor r_a = 6.1 ohm

   Armature resistance of the d.c. machine = 5.31 ohms.

APPENDIX C1

```
C       MEASUREMENT OF XD,XQ,PL OF MACHINE
        DIMENSION V(20),AI1(20),P1(20),AI2(20),P2(20),PL(20),
        1S(20),VP(20),VF(20),XD1(20),XQ1(20),XD(20),XQ(20),F(20),
        2Z(20),PF(20),PF1(20),X(20),G(20),R1(20)
        OPEN(UNIT=1,DEVICE='DSK', FILE='IN.DAT')
        OPEN (UNIT=2,DEVICE='DSK', FILE='OUT.DAT')
        R=6.14
        DO 100 J=1,19
        READ(1,*) V(J), AI1(J),P1(J),AI2(J),P2(J),S(J)
        PRINT 9 , V(J),AI1(J),AI2(J),P1(J),P2(J),S(J)
9       FORMAT (/2X,6(F8.2,2X)/)
        F(J)=S(J)/1500.
        VP(J)=V(J)/SQRT(3.)
        VF(J)=VP(J)/F(J)
        XD1(J)=SQRT((VP(J)/AI1(J))**2-R**2)
        Z(J)=VP(J)/AI2(J)
        PF(J)=P2(J)/(3.*VP(J)*AI2(J))
        PF1(J)=ACOS(PF(J))
        R1(J)=Z(J)*PF(J)
        X(J)=Z(J)*SIN(PF1(J))
        PL(J)=P1(J)-3.*AI1(J)**2*R
        G(J)=PL(J)/(3.*VP(J)**2)
        XQ1(J)=(X(J)*(XD1(J)-X(J))-(R1(J)-R)**2)/
        1((1.+G(J)*(G(J)*Z(J)**2-2.*R1(J)))*XD1(J)-X(J))
        XD(J)=XD1(J)/F(J)
        XQ(J)=XQ1(J)/F(J)
        WRITE (2,*)V(J), VP(J),VF(J),XD1(J),XQ1(J)
        1,XD(J),XQ(J),PL(J)
100     CONTINUE
        STOP
        END
```

APPENDIX C2

```
C     NO LOAD PERFORMANCE OF RELUCTANCE MOTOR
      VB=400/1.73
      AIB=2.5
      ZB=VB/AIB
      FB=50.
      RA=6.07
      B1=15.
      PAI=22./7.
      B=PAI*B1/180.
      DF1=.1
      DO 12 IC =10,80,10
      C=IC
      DO 12 IVD=100,420,20
      VD=IVD
      DF=DF1
      FBB=10000.0
      K2=0 ;K3=0
      XC=(10.**6)/(2.*PAI*C*FB)
      VP=PAI*VD/(3*COS(B)*SQRT(6.))
      V=VP/VB
      F=0.3
      K=0
22    VF=VP/F
      K=K+1
      IF (VF.GT.204.) GO TO 25
      BK1=383.33 ; BK2=1.333
      XD=BK1-BK2*VF
      GO TO 36
25    IF (VF.GT.270.) GO TO 26
      BK3=290.77 ; BK4=0.923
      XD=BK3-BK4*VF
      GO TO 36
26    XD=40.
36    XD1=F*XD
      IF (VF.GT.200.) GO TO 55
      CK1=163.39 ; CK2=0.63
      XQ=CK1-CK2*VF
```

```
      GO TO 46
55    IF (V.GT.260.) GO TO 56
      CK3=23.5 ; CK4=0.4375
      XQ=CK3-CK4*VF
      GO TO 46
56    XQ=1.
46    XQ1=F*XQ
      AKX=XD1/XQ1
      AKR=RA/XQ1
      AKC=XC/XQ1
      IF(VF.LT.195.) GO TO 15
[redacted]
17    PL=50.
16    A5=3.*VP**2*(XD1-XQ1)/(2.*(XD1*XQ1+RA**2)**2)
      A1=RA*A5*(XD1+XQ1)
      A2=A5*(XD1*XQ1-RA**2)
      A3=A5*RA*(XD1-XQ1)+PL
      A4=SQRT(A1**2+A2**2)
      DLM=.5*ATAN(A2/A1)
      DL=DLM-.5*ACOS(A3/A4)
      AF1=F*(AKX+AKR**2)
      AF2=AKC*SQRT((COS(DL)-AKR*SIN(DL))**2+(AKX*SIN(DL)+AKR
     1*COS(DL))**2-.25*((AKX-1)*SIN(2.*DL)+2.*AKR)**2)
      AF3=.5*AKC*(SIN(B)/COS(B))*(AKX-1)*SIN(2.*DL)
      AF4=AKC*AKR*(SIN(B)/COS(B))
      FF=AF1-AF2-AF3-AF4
       WRITE(1,30)  FF,F,XD1,XQ1,DL,PL,XC
C     FORMAT(/2X,7(F11.4,2X)/)
CO    IF(ABS(FF).GE.FBB) GO TO 200
      DLB=DL
      FBB=ABS(FF)
```

```
              FFB=F
              DF=3.*DF
              K3=K3+1
              GO TO 300
       200    DF=-0.5*DF
       C       FFB=F
              K2=K2+1
       300    F=FFB+DF
              IF(K.GT.100) GO TO 20
              IF(ABS(FBB).LT..01) GO TO 20
              GO TO 22
       20     F1=FFB*FB
              F=FFB
              XD1=F*XD ; XQ1=F*XQ
              AN=30.*F1
              PI=3.*VP**2*((XD1-XQ1)*SIN(2.*DLB)+2.*RA)/(2.*(XD1*XQ1+RA
              1**2))
              PRINT9,C,VD,VP,VF,FFB,FBB,F1,AN
       9      FORMAT(///,8(F11.5,3X)/)
              PRINT*,K,K2,K3,F,FF,DF,PL,XC,B1
              FF=((AKX-1)*SIN(2.*DLB)+2.*AKR)/
              1SQRT(2.*((AKX**2-1.)+2.*AKR*(AKX-1.)*SIN(2.*DLB)-
              2(AKX**2-1.)*COS(2.*DLB)+2.*(AKR**2+1.)))
              AIC=SQRT(3.)*VP*F/XC
              AID=PI/VD
              AIM=PI/(3.*VP*PF)
              PRINT 11,AIC,AID,AIM,XD,XQ,DL,PI,PF
       11     FORMAT(/1X,8(F10.4,3X))
       12     CONTINUE
              STOP
              END
```

APPENDIX C2

```
        FFB=F
        DF=3.*DF
        K3=K3+1
        GO TO 300
200     DF=-0.5*DF
C        FFB=F
        K2=K2+1
300     F=FFB+DF
        IF(K.GT.100) GO TO 20
        IF(ABS(FBB).LT..01) GO TO 20
        GO TO 22
20      F1=FFB*FB
        F=FFB
        XD1=F*XD ; XQ1=F*XQ
        AN=30.*F1
        PI=3.*VP**2*((XD1-XQ1)*SIN(2.*DLB)+2.*RA)/(2.*(XD1*XQ1+RA
        1**2))
        PRINT9,C,VD,VP,VF,FFB,FBB,F1,AN
9       FORMAT(///,8(F11.5,3X)/)
        PRINT*,K,K2,K3,F,FF,DF,PL,XC,B1
        PF=((AKX-1)*SIN(2.*DLB)+2.*AKR)/
        1SQRT(2.*((AKX**2-1.)+2.*AKR*(AKX-1.)*SIN(2.*DLB)-
        2(AKX**2-1.)*COS(2.*DLB)+2.*(AKR**2+1.)))
        AIC=SQRT(3.)*VP*F/XC
        AID=PI/VD
        AIM=PI/(3.*VP*PF)
        PRINT 11,AIC,AID,AIM,XD,XQ,DL,PI,PF
11      FORMAT(/1X,8(F10.4,3X))
12      CONTINUE
        STOP
        END
```

APPENDIX C3

```
C      PERFORMANCE OF RELUCTANCE MOTOR WITH LOAD
       VB=400/1.73
       AIB=2.5
       ZB=VB/AIB
       FB=50.
       RA=6.07
       B1=20.
       PAI=22./7.
       B=PAI*B1/180.
       DF1=.1
C      DO 12 IVD=120,240,20
C      VD =IVD
C      DO 12 IC=10,80,10
C      C=IC
C      C=70.0 ; VD=220.0
       C=30.0 ; VD=340.0
       DO 12 IPO=10,300,10
       PO=IPO-10
       DF=DF1
       FBB=10000.0
       K2=0 ;K3=0
       XC=(10.**6)/(2.*PAI*C*FB)
       VP=PAI*VD/(3*COS(B)*SQRT(6.))
       V=VP/VB
       F=0.3
       K=0
22     VF=VP/F
       K=K+1
       IF (VF.GT.204.) GO TO 25
       BK1=383.33 ; BK2=1.333
       XD=BK1-BK2*VF
       GO TO 36
25     IF(VF.GT.270.) GO TO 26
       BK3=290.77 ; BK4=.923
       XD=BK3-BK4*VF
       GO TO 36
26     XD=40.
```

```
36    XD1=F*XD
      IF (VF.GT.200.) GO TO 55
      CK1=163.39 ;CK2=.637
      XQ=CK1-CK2*VF
      GO TO 46
55    IF (VF.GT.260.) GO TO 56
      CK3=123.5 ; CK4=0.4375
      XQ=CK3-CK4*VF
      GO TO 46
56    XQ=10.
46    XQ1=F*XQ
      AKX=XD1/XQ1
      AKR=RA/XQ1
      AKC=XC/XQ1
      IF (VF.LT.195.)GO TO 15
      AK1=-548.275 ; AK2=3.659
      PL=AK1+AK2*VF
      GO TO 16
15    IF (VF.LT.80.) GO TO 17
      AK3=-33.6 ; AK4=1.05
      PL=AK3+AK4*VF
      GO TO 16
17    PL=50.
16    A5=3.*VP**2*(XD1-XQ1)/(2.*(XD1*XQ1+RA**2)**2)
      A1=RA*A5*(XD1+XQ1)
      A2=A5*(XD1*XQ1-RA**2)
      A3=A5*RA*(XD1-XQ1)+PL
      A4=SQRT(A1**2+A2**2)
      DLM=.5*ATAN(A2/A1)
      POM=3.*VP**2*(XD1-XQ1)*((XD1*XQ1-RA**2)*
      1SIN(2.*DLM)+RA*(XD1+XQ1)*COS(2.*DLM)-RA*(
      2XD1-XQ1))/(2.*(XD1*XQ1+RA**2)**2)-PL
      IF(PO.GT.POM) GO TO 200
      DL=DLM-.5*ACOS((PO+A3)/A4)
      DL1=DLM-.5*ATAN((SQRT(A4**2+(PO+A3)**2)/(PO+
      1A3)))
      AF1=F*(AKX+AKR**2)
```

APPENDIX C3

```
      AF2=AKC*SQRT((COS(DL)-AKR*SIN(DL))**2+(AKX*SIN(DL)+AKR
      1*COS(DL))**2-.25*((AKX-1)*SIN(2.*DL)+2.*AKR)**2)
      AF3=.5*AKC*(SIN(B)/COS(B))*(AKX-1)*SIN(2.*DL)
      AF4=AKC*AKR*(SIN(B)/COS(B))
      FF=AF1-AF2-AF3-AF4
C      PRINT 30,  FF,F,XD1,XQ1,DL,PL,XC
C0    FORMAT(/2X,7(F11.4,2X)/)
      IF(ABS(FF).GE.FBB) GO TO 200
      DLB=DL
      FBB=ABS(FF)
      FFB=F
      DF=3.*DF
      K3=K3+1
      GO TO 300
200   DF=-0.5*DF
      K2=K2+1
300   F=FFB+DF
      IF(K.GT.500) GO TO 20
      IF(ABS(FBB).LT..01) GO TO 20
      GO TO 22
20    F1=FFB*FB
      F=FFB
      XD1=F*XD ; XQ1=F*XQ
      AN=30.*F1
      PI=3.*VP**2*((XD1-XQ1)*SIN(2.*DLB)+2.*RA)/(2.*(XD1*XQ1+RA
      1**2))
      T=30.*PO/(PAI*AN)
      PRINT 9,C,VD,VP,VF,FFB,FBB,F1,XC,AN,T
9     FORMAT(///,10(F9.3,2X)/)
      PRINT*,K,K2,K3,F,FF,DF,PL,XD,XQ,POM,B1
      PF=((AKX-1)*SIN(2.*DLB)+2.*AKR)/
      1SQRT(2.*((AKX**2-1.)+2.*AKR*(AKX-1.)*SIN(2.*DLB)-
      2(AKX**2-1.)*COS(2.*DLB)+2.*(AKR**2+1.)))
      AIC=SQRT(3.)*VP*F/XC
      AID=PI/VD
      AIM=PI/(3.*VP*PF)
      EFF=PO/PI
```

```
      PRINT 11,AID,AIC,AIM,DLM,DL,DL1,PI,PF,PO,EFF
11    FORMAT(/1X,10(F8.3,1X)//)
12    CONTINUE
      STOP
      END
```